

Bulk 3
date

WANL-PR(Q)-007
NASCR-54658

NASA

N 66-15342

FACILITY FORM 602

(ACCESSION NUMBER)	(THRU)
72	1
(PAGES)	(CODE)
OR 54658	17
(NASA OR TMA OR ID NUMBER)	(CATEGORY)

GPO PRICE \$ _____

CFSTI PRICE(S) \$ _____

Hard copy (HC) 3.00

Microfiche (MF) 75

ff 653 July 65

DEVELOPMENT OF DISPERSION STRENGTHENED TANTALUM BASE ALLOY

Sixth Quarterly Report

by

R. W. Buckman, Jr. and R.C. Goodspeed

prepared for
National Aeronautics and Space Administration
Lewis Research Center
Space Power Systems Division
Under Contract (NAS 3-2542)



Astronuclear Laboratory
Westinghouse Electric Corporation

NOTICE

This report was prepared as an account of Government-sponsored work. Neither the United States nor the National Aeronautics and Space Administration (NASA), nor any person acting on behalf of NASA:

- A) Makes any warranty or representation, expressed or implied, with respect to the accuracy, completeness, or usefulness of the information contained in this report, or that the use of any information apparatus, method, or process disclosed in this report may not infringe privately-owned rights; or
- B) Assumes any liabilities with respect to the use of, or for damages resulting from the use of any information, apparatus, method or process disclosed in this report.

As used above, "person acting on behalf of NASA" includes any employee or contractor of NASA, or employee of such contractor, to the extent that such employee or contractor of NASA or employee of such contractor prepares, disseminates, or provides access to, any information pursuant to his employment or contract with NASA, or his employment with such contractor.

Copies of this report can be obtained from:

National Aeronautics & Space Administration
Office of Scientific and Technical Information
Washington 25, D. C.
Attention: AFSS-A

DEVELOPMENT OF DISPERSION STRENGTHENED
TANTALUM BASE ALLOY

by

R. W. Buckman, Jr.

and

R. C. Goodspeed

SIXTH QUARTERLY PROGRESS REPORT

Covering the Period

February 20, 1965 - May 19, 1965

Prepared For

NATIONAL AERONAUTICS AND SPACE ADMINISTRATION

Contract NAS 3-2542

Technical Management

Paul E. Moorhead

NASA - Lewis Research Center

Space Power Systems Division

Astronuclear Laboratory

Westinghouse Electric Corporation

Pittsburgh 36, Pa.

ABSTRACT

15343

Development of dispersion strengthened tantalum base alloys for use in advanced space power systems continued with the melting of the first 4-inch diameter ingot sheet and tubing alloy composition (Ta-8W-1Re-0.7Hf-0.025C). Three additional alloys were produced into 2-inch diameter ingots as part of the composition optimization phase of the program. Six of the planned seven ingots to be produced for this optimization study are in various stages of preparation and evaluation. Phase identification and morphology studies were initiated on a number of alloys using optical and electron microscopy, x-ray, and electron diffraction techniques, and electron beam microprobe analysis. Metallographic procedures for these alloys are detailed.

Author

TABLE OF CONTENTS

	<u>Page</u>
I. INTRODUCTION	1
II. PROGRAM STATUS	2
A. OPTIMIZATION INVESTIGATION	2
B. FOUR-INCH DIAMETER INGOT SCALE-UP	10
C. TURBINE COMPOSITIONS	17
D. PHASE IDENTIFICATION AND MORPHOLOGY	17
III. FUTURE WORK	40
IV. REFERENCES	42
APPENDIX I	43
APPENDIX II	44
APPENDIX III	47

LIST OF TABLES

	<u>Page</u>
1. Melting Data for Compositions NASV-15, NASV-16, and NASV-17	3
2. Results of Upset Forging of Compositions NASV-15 and NASV-16	3
3. Chemical Analysis of Compositions NASV-12, NASV-13, and NASV-14	4
4. Ductile-Brittle Transition Temperatures of Compositions NASV-12, NASV-13, and NASV-14	6
5. Tensile Properties of Compositions NASV-12, NASV-13, and NASV-14	9
6. Creep Results on Compositions NASV-12 and NASV-13 at 1×10^{-8} Torr	10
7. First Melt Data for Composition NASV-20	11
8. Second Melt Data for Composition NASV-20	11
9. Chemical Analysis Data of First Melt Electrode Composition NASV-20	15
10. Mechanical Properties of NASV-11	18
11. Results of X-ray Diffraction Analyses on Samples of Composition NASV-9	22
12. Results of X-ray Diffraction Analyses on Samples of Composition NASV-7	33

LIST OF FIGURES

	<u>Page</u>
1. Schematic of Second Melt Electrode of Composition NASV-20	12
2. Second Melt Electrode of Composition NASV-20	13
3. Four Inch Diameter Ingot and Second Melt Electrode Adaptor of Composition NASV-20	14
4. Macrostructure of Four Inch Diameter Ingot of Composition NASV-20	16
5. Optical and Electron Micrographs of Creep Specimens of Composition NASV-9	24
6. 1315°C (2400°F) Isotherm of Tantalum Corner of (Ta,W)-Hf-C Pseudo Ternary System	26
7. Optical and Electron Micrographs of T-111	28
8. Optical and Electron Micrographs of Creep Specimens of Composition NAS-56	29

LIST OF FIGURES

	<u>Page</u>
9. Optical Micrographs of Creep Specimens of Composition NASV-7	35
10. Electron Micrographs of Creep Specimen T-1C of Composition NASV-7	36
11. Electron Micrographs of Creep Specimen T-5C of Composition NASV-7	37
12. Transmission Electron Micrographs of Precipitates Extracted from Creep Specimen T-5C of Composition NASV-7	38
13. Optical and Electron Microscopy of Creep Specimen M-2C of Composition NASV-8	41

I. INTRODUCTION

This, the Sixth Quarterly Progress Report on the NASA sponsored program, "Development of a Dispersion Strengthened Tantalum Base Alloy", describes the work accomplished during the period February 20, 1965 to May 19, 1965. This work was performed under Contract NAS-3-2542.

The primary objective of this Phase II work is the double vacuum arc melting of three optimized compositions into 60-pound, 4-inch diameter ingots. These compositions are to be selected for a combination of weldability, creep resistance, and fabricability since the primary use will be as sheet and tubing.

Prior to this quarterly period, several promising tantalum alloy compositions were developed⁽¹⁾. These alloys exhibited good resistance to creep deformation at 1315°C (2400°F) while still retaining adequate fabricability and weldability. From these alloys, a weldable sheet and tubing composition NASV-20 (Ta-8W-1Re-0.7Hf-0.025C) was chosen as one of three compositions for the 4-inch diameter Phase II ingots, and melting was initiated. Selection of this composition was possible since the major emphasis in Phase I was on the carbide dispersion strengthened system. Seven additional 2-inch diameter ingot compositions were selected to be evaluated for fabricability, weldability, and creep strength before composition selection and melting of the remaining two 4-inch diameter ingots. These ingots are to optimize the carbo-nitride dispersion strengthened system. Three of these compositions were melted and are in various stages of evaluation.

During this quarterly period, melting of NASV-20 (Ta-8W-1Re-0.7Hf-0.025C) was completed and preparation of the ingot for fabricability studies was initiated. Three additional 2-inch diameter ingots were melted and now six of the seven compositions are in various stages of preparation and evaluation. Phase identification and morphology studies were continued in more detail on a number of the alloy compositions using optical and electron microscopy, x-ray and electron diffraction, and electron beam microprobe analysis.

II. PROGRAM STATUS

A. OPTIMIZATION INVESTIGATION

The optimization compositions are being double vacuum AC arc-melted into 2-inch diameter ingots and are being processed to 0.04-inch sheet and evaluated as to weldability, creep resistance, and fabricability.

Melting — First melt electrodes of compositions NASV-15,^{*} NASV-16 and NASV-17 were assembled using the sandwich technique previously described⁽¹⁾. The first melts were made into 1-5/16-inch diameter molds and these melts were subsequently melted into 2-inch diameter molds. Melt data for these compositions are recorded in Table 1. All three 2-inch diameter as-melted ingots had excellent sidewalls.

Primary Breakdown — A 3/4-inch slice was removed from the bottom portion of the NASV-15 and NASV-16 ingots. These slices were then coated with an Al-12Si alloy and upset forged at 1300°C (2372°F) on the Dynapak. Composition NASV-16 forged satisfactorily, while composition NASV-15 exhibited some surface and edge cracking. The forging results are reported in Table 2.

The balance of ingots NASV-12, NASV-13, NASV-14, and NASV-16 were plasma sprayed with unalloyed molybdenum and extruded at 1400°C (2550°F) to sheet bar (4:1 reduction ratio). The balance of ingot NASV-15 was also plasma sprayed with unalloyed molybdenum and extruded at the same temperature to a 1-inch diameter round bar. It will be evaluated for possible turbine application rather than for the sheet and tubing application originally intended.

Composition NASV-17 is presently being prepared for upset forging and extrusion to sheet bar.

*Compositions and corresponding heat numbers are listed in Appendix I.

TABLE 1 - Melting Data for Compositions NASV-15, NASV-16, and NASV-17

Composition	Melt	Melt Voltage (volts)	Melt Power (kw)	Melt Rate (lbs./min.)
Ta-9W-1.5Re-1Hf-0.06N (NASV-15)	First	21-22	45	2.35
	Second	23	60	3.50
Ta-9.5W-0.5Re-0.25Zr-0.02C-0.01N (NASV-16)	First	21-22	45	2.23
	Second	25	60-65	3.51
Ta-4W-3Re-0.75Hf-0.01C-0.02N (NASV-17)	First	22	43	2.46
	Second	22-25	50-60	4.25

TABLE 2 - Results of Upset Forging of Compositions NASV-15 and NASV-16

Composition	As-Cast Hardness DPH (30 Kg Load)	Forging Temperature (°C/°F)	Reduction (%)	Upset Constant (K _u) ^(a) (psi)
Ta-9W-1.5Re-1Hf-0.06N (NASV-15)	370	1300/2372	61	138,500
Ta-9.5W-0.5Re-0.25Zr-0.02C-0.01N (NASV-16)	321	1300/2372	64	148,500

(a) $K_u = \frac{E}{VZ}$ where: E = energy used
V = volume of material deformed
Z = upset factor

Secondary Working — The extruded sheet bars of compositions NASV-12, NASV-13, NASV-14, and NASV-16, and the forged section of composition NASV-16 were conditioned, annealed for one hour at 1650°C (3000°F), and then processed to 0.04-inch sheet using established practice. High quality sheet was obtained in all cases. The forged section of composition NASV-15 was annealed for two hours at 1800°C (3270°F) prior to rolling at 500°C (930°F). Severe cracking occurred after a reduction of only 15 to 20 percent. It is for this reason that it was decided to further process the remaining ingot into 0.4-inch diameter rod and evaluate its potential for turbine applications.

Chemical Analysis — Chemical analyses obtained on compositions NASV-12, NASV-13, and NASV-14, are reported in Table 3. Samples for the analyses of metallic elements were obtained from the bottom portion of the as-cast ingots and samples for the analysis of interstitial elements were obtained from 0.04-inch thick sheet processed from the forged section (bottom) of the ingots. Analysis of the interstitial elements are also being obtained on sheet processed from the extruded ingots.

TABLE 3 - Chemical Analysis of Compositions NASV-12, NASV-13, and NASV-14

Composition	Analysis (weight percent)				
	W	Re	Mo	C	N
Ta-7.5W-1.5Re-0.5Hf-0.015C-0.015N (NASV-12)	7.9	1.52	---	0.019	0.011
Ta-6.5W-2.5Re-0.3Hf-0.01C-0.01N (NASV-13)	6.3	2.57	---	0.011	0.012
Ta-4W-1Mo-2Re-0.3Zr-0.015C-0.015N (NASV-14)	4.0	2.05	1.01	0.016	0.013

Weldability — The ductile-brittle transition temperatures for TIG and EB welded sheet are summarized in Table 4 for compositions NASV-12, NASV-13, and NASV-14. Welds were made on 0.04-inch thick sheet in both the as-worked and annealed (1 hour at 1650°C/3000°F) conditions. Also included in Table 4 are the ductile-brittle transition temperatures of base metal sheet samples processed from extruded ingots for all three compositions and from forged ingots for NASV-12 and NASV-13, again in both the as-worked and annealed conditions. The bend transition temperature of the three compositions (in both conditions) as determined from base metal sheet samples processed from extrusions ranged from -175°F (-115°C) to less than -320°F (-195°C). Consistent with past experience, EB welding had little effect on the transition temperature while TIG welding increased it significantly.

Mechanical Property Evaluation — Room temperature and elevated temperature tensile properties were determined for compositions NASV-12, NASV-13, and NASV-14 (see Table 5). All test specimens were annealed for one hour at 1650°C (3000°F) prior to testing.

Creep tests in ultra-high vacuum were initiated on compositions NASV-12 and NASV-13. The results are reported in Table 6. These specimens were also annealed for one hour at 1650°C (3000°F) prior to testing. Composition NASV-12 is especially noteworthy. No measurable plastic strain occurred during 257.8 hours at 1315°C (2400°F) under an applied stress of 10,000 psi and only 0.01 percent plastic strain occurred during 210.2 hours at the same temperature under an applied stress of 15,000 psi. The extrapolated time required to reach 1 percent plastic strain at 1315°C (2400°F) under a nominal stress of 15,000 psi is considerably greater for this composition than for any other tantalum alloy evaluated to date. Creep testing is continuing on both NASV-13 and NASV-14 at 1425°C (2600°F).

Tensile and creep specimens have been machined from NASV-16, annealed for one hour at 1650°C (3000°F), and are now ready for testing.

TABLE 4 - Ductile-Brittle Transition Temperatures of Compositions
NASV-12, NASV-13, and NASV-14^(a)

Composition	Condition	Temperature (°F/°C)	No Load Bend Angle (degrees)	Remarks
Ta-7.5W-1.5Re- 0.5Hf-0.015C- 0.015N (NASV-12)	Base Metal ^(b) As-Worked 1 Hr./1650°C	-225/-143	94	Bend*
		-250/-157	31	Break
		-175/-115	96	Bend
		-200/-129	66	Break
	Base Metal ^(c) As-Worked 1 Hr./1650°C	-150/-101	91	Bend
		-200/-129	90	Break
		-175/-115	96	Bend
		-200/-129	90	Break
	Electron Beam Welded ^(b) As-Worked 1 Hr./1650°C	-200/-129	94	Bend
		-225/-143	35	Break
		-200/-129	96	Bend
		-225/-143	25	Break
	TIG Welded ^(b) As-Worked 1 Hr./1650°C	0/-18	96	Bend**
		-25/-32	35	Break
		0/-32	96	Bend*
		-25/-32	96	Break

**TABLE 4 - Ductile-Brittle Transition Temperatures of Compositions
NASV-12, NASV-13, and NASV-14(a)
(continued)**

Composition	Condition	Temperature (°F/°C)	No Load Bend Angle (degrees)	Remarks
Ta-6.5W-2.5Re- 0.3Hf-0.01C- 0.01N (NASV-13)	Base Metal ^(b) As-Worked 1 Hr./1650°C	-250/-157	91	Bend*
		-320/-195	55	Break
		-250/-157	94	Bend*
		-320/-195	35	Break
	Base Metal ^(c) As-Worked 1 Hr./1650°C	-250/-157	91	Bend*
		-320/-195	50	Break
		-225/-143	91	Bend*
		-250/-157	25	Break
	Electron Beam Welded ^(b) As-Worked 1 Hr./1650°C	-225/-143	91	Bend
		-250/-157	55	Break
		-225/-143	90	Bend
		-250/-157	40	Break
	TIG Welded ^(b) As-Worked 1 Hr./1650°C	-100/-73	94	Bend*
		-200/-129	80	Break
		-150/-101	94	Bend*
		-200/-129	31	Break

TABLE 4 - Ductile-Brittle Transition Temperatures of Compositions
NASV-12, NASV-13, and NASV-14(a)
(continued)

Composition	Condition	Temperature (°F/°C)	No Load Bend Angle (degrees)	Remarks
Ta-4W-1Mo- 2Re-0.3Zr-0.015 C-0.015N (NASV-14)	Base Metal ^(b)			
	As-Worked	-320/-195	91	Bend
	1 Hr./1650°C	-320/-195	91	Bend
		-200/-129	95	Bend
		-225/-143	60	Break
	Electron Beam Welded ^(b)			
	As-Worked	-225/-143	91	Bend
	1 Hr./1650°C	-250/-157	56	Break
		-175/-115	96	Bend
		-200/-129	30	Break
	TIG Welded ^(b)			
	As-Worked	+RT/24	96	Bend
		+50/10	75	Break
		+25/-4	96	Bend*
		0/-18	25	Break

(a) Bend radii - 1.8t

(b) Plate processed from extruded ingot

(c) Plate processed from forged ingot

* Sample exhibited ductile fracture in base metal

** Base metal failure

TABLE 5 - Tensile Properties of Compositions NASV-12, NASV-13, and NASV-14^(c)

Composition	Test Temperature (°F/°C)	0.2% Yield Strength (psi)	Ultimate Tensile Strength (psi)	% Elongation Uniform	% Elongation Total	% Reduction in Area
Ta-7.5W-1.5Re-0.5Hf-0.015C-0.015N (NASV-12)	R. T./25 ^(a)	132,200	138,800	8.6	15.3	55.0
	2200/1205 ^(b)	38,100	56,500		25.3	
	2400/1316 ^(b)	32,200	44,900		28.7	
	2600/1427 ^(b)	31,300	37,500		36.0	
	2800/1538 ^(b)	25,400	28,900		49.5	
Ta-6.5W-2.5Re-0.3Hf-0.01C-0.01N (NASV-13)	R. T./25 ^(a)	142,000	146,300	6.5	12.7	57.5
	2200/1205 ^(b)	39,900	53,800		26.5	
	2400/1316 ^(b)	32,300	42,800		31.2	
	2600/1427 ^(b)	30,300	35,300		37.6	
	2800/1538 ^(b)	22,900	26,000		42.5	
Ta-4W-1Mo-2Re-0.3Zr-0.015C-0.015N (NASV-14)	R. T./25 ^(a)	138,200	142,700	10.4	17.3	55.1
	2200/1205 ^(b)	39,300	62,400		20.1	
	2400/1316 ^(b)	37,000	51,500		27.9	

- (a) Strain rate 0.005 in/in/min. through 0.6% yield and then 0.05 in/in/min. for balance of test.
 (b) Strain rate of 0.05 in/in/min. throughout test.
 (c) Annealed for 1 hour at 1650°C (3000°F) prior to test.

TABLE 6 - Creep Results on Compositions NASV-12 and NASV-13
at 1×10^{-8} Torr

Composition/Heat No.	Test Temperature (°C/°F)	Stress (psi)	Test Duration (hrs.)	Total Plastic Strain (%)	Creep Rate (% per hr.)
Ta-7.5W-1.5Re-0.5Hf -0.015C-0.015N (NASV-12)	1315/2400	15,000	210.2	0.01	0.00047
	1315/2400	10,000	257.8	0.0	---
	1315/2400	20,180	171.1	7.93	0.0286
	1425/2600	8,000	512.9	0.89	0.0017
Ta-6.5W-2.5Re-0.3Hf -0.01C-0.01N (NASV-13)	1315/2400	15,000	354.8	0.39	0.0011
	1315/2400	10,000	283.6	0.2	0.0007

B. FOUR-INCH DIAMETER INGOT SCALE-UP

Significant progress was made in the processing of composition NASV-20 (Ta-8W-1Re-0.7Hf-0.025C) which was selected as a carbide dispersion strengthened sheet and tubing alloy.

Melting — The first melt, started during the last quarterly period⁽²⁾ was completed by melting the last section of electrode (i.e., the second half of the second electrode) into a 2-1/2-inch diameter water-cooled copper mold using AC vacuum arc melting practice. First melt data, including that of the three sections previously melted, are recorded in Table 7. The four first-melt ingots were then conditioned, studded, and welded together. The resulting 84.5 pound second-melt electrode, shown in Figures 1 and 2 was 2.4 inches in diameter and 33-7/8 inches in length.

The 2.4-inch diameter first-melt electrode was then melted into a 4-inch diameter water-cooled copper mold, using DC vacuum arc melting practice. The melting data are recorded in Table 8. Figure 3 illustrates the resulting ingot and its excellent sidewalls.

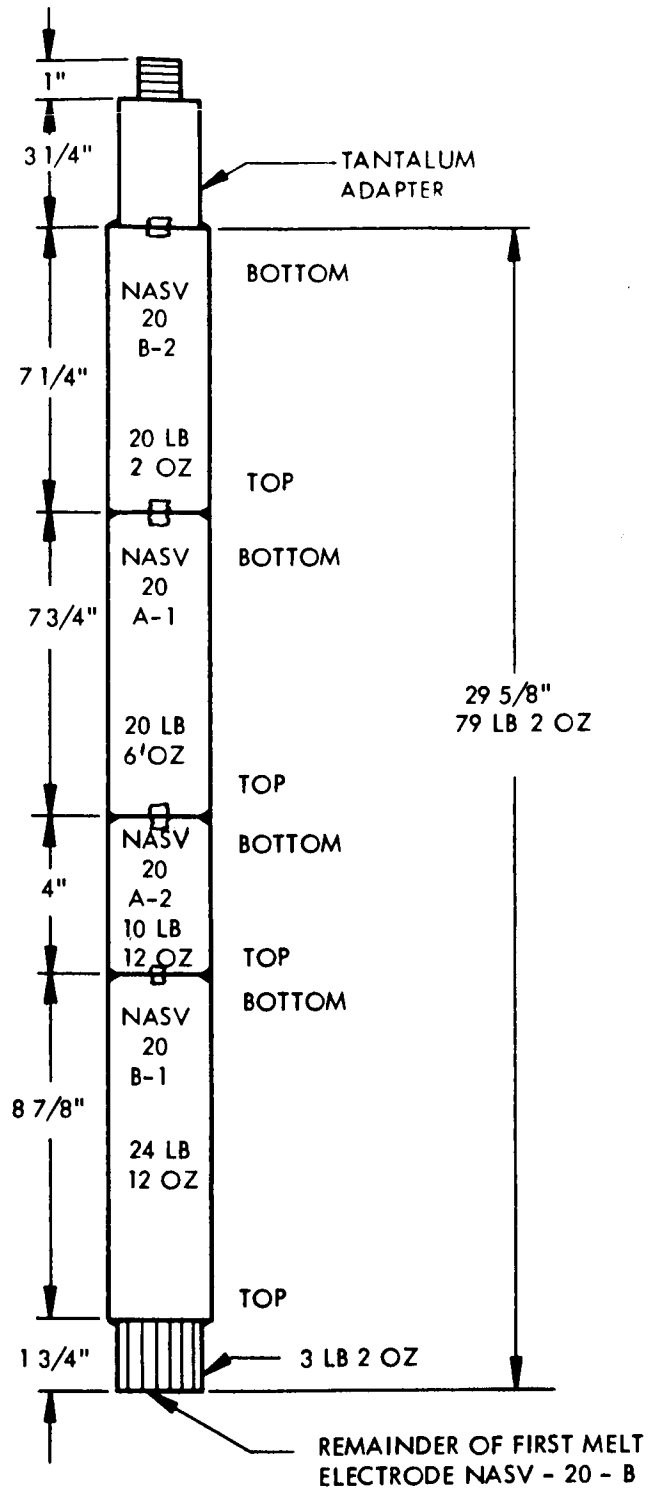
TABLE 7 - First Melt Data for Composition NASV-20
(Ta-8W-1Re-0.7Hf-0.025C)

Electrode	Arc Voltage (volts)	AC Power (kw)	Melt Rate (lbs/min)	Ingot Condition
NASV-20A1	29	95	6.12	Good
NASV-20A2	28-29	95	6.35	Good
NASV-20B1	28-29	95-100	6.45	Good
NASV-20B2	29	95-100	6.05	Good

TABLE 8 - Second Melt Data for Composition NASV-20
(Ta-8W-1Re-0.7Hf-0.025C)

Time (min.)	Arc Voltage (volts)	DC Melt Power (kw)	Melt Rate (lbs/min)
Arc Started	30	90	3.49
1	30	114	
2	30	138	
3	30	150	
4	30	165	
5	30	175	
6 through 16	30	175	
17	30	170	
17.5 (Start of Hot Top)	28	158	
18.5	28	150	
19.5	28	150	
20.5	25	90	
21.5	20	55	
22.5	20	48	

Pressure during melting was 5×10^{-4} mm Hg.



605946-A

FIGURE 1 - Schematic of Second Melt Electrode of Composition NASV-20
(Ta-8W-1Re-0.7Hf-0.025C)

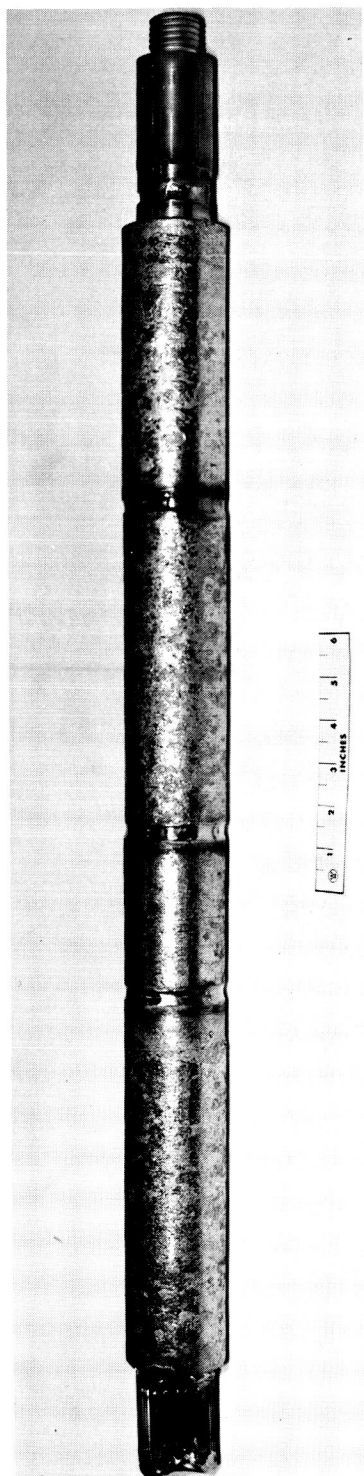


FIGURE 2 - Second Melt Electrode of Composition NASV-20
(Ta-8W-1Re-0.7Hf-0.025C)



FIGURE 3 - Four Inch Diameter Ingot and Second Melt Electrode Adaptor of Composition NASV-20 (Ta-8W-1Re-0.7Hf-0.025C)

After conditioning, the ingot measured 3.875 inches in diameter by 10-1/2 inches in length and weighed 74-1/2 pounds.

Primary Breakdown — The conditioned ingot sectioned into three parts:

1. A 3.9-inch diameter x 1-inch long section cut from the bottom end of the ingot is being coated with Al-12Si alloy and will be upset forged at 1200-1400°C (2200-2550°F).
2. A 3.9-inch diameter x 5-inch long section from the middle of the ingot is being similarly coated and will be side forged at 1200-1400°C (2200-2550°F).
3. A 3.9-inch diameter x 4-inch long section from the top of the ingot will be canned in either molybdenum or mild steel and extruded to sheet bar at a temperature yet to be selected.

The as-cast macrostructure, obtained about 1 inch from the bottom of the ingot, is shown in Figure 4. A hardness traverse, taken on the same surface, indicated an average diamond pyramid hardness (for a 30 Kg load) of 237. The range of hardness values was less than 15 percent of the average value.

Chemical Analysis — Chemical analyses were made on samples obtained from the central axis of one of the first melt ingots and from the outside of a second first melt ingot. The results are recorded in Table 9. Chemical analyses are also being obtained for metallic and interstitial elements on samples taken from both ends of the 4-inch diameter ingot.

TABLE 9 - Chemical Analysis Data of First Melt Electrode Composition NASV-20
(Ta-8W-1Re-0.7Hf-0.025C)

Position	(Analysis, weight percent)					
	W		Re		Hf	
	Actual	Nominal	Actual	Nominal	Actual	Nominal
Center Axis	7.8	8.0	1.00	1.0	0.68	0.7
Outside Surface	7.5	8.0	1.04	1.0	0.71	0.7

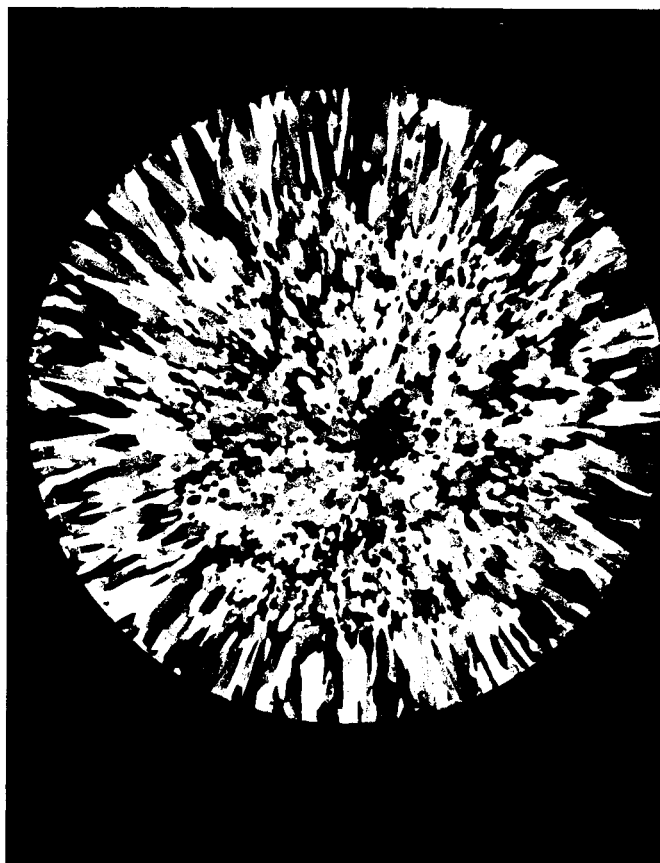


FIGURE 4 - Macrostructure of Four Inch Diameter Ingot of
Composition NASV-20. (Ta-8W-1Re-0.7Hf-0.025C)
Mag. 0.8 X

C. TURBINE COMPOSITIONS

Although it was originally planned to make one of the 4-inch ingots a turbine (or bar type) composition, the present plans do not call for scale up of the 2-inch diameter ingot compositions. To date two compositions have been melted as 2-inch diameter ingots, fabricated and processed for evaluation as potential turbine materials. They are NASV-10 (Ta-7.1W-1.56Re-0.25Hf-0.12Zr-0.03N) and NASV-11 (Ta-9W-1.5Re-1Hf-0.015C-0.015N). A third composition NASV-15 (Ta-9W-1.5Re-1Hf-0.06N) is presently being considered for turbine applications also, because of the difficulties encountered in reducing it to sheet. Melting, primary working, and secondary breakdown of NASV-15 were previously discussed under the "Optimization Investigation" section of this report. The NASV-15 1-inch diameter extrusion has been hot straightened (by swaging at about 1200°C/2190°F) and centerless ground in preparation for swaging to 0.4-inch diameter rod.

Mechanical Property Evaluation — Tensile properties were obtained on NASV-11 specimens which were annealed for one hour at 1650°C (3000°F) prior to testing. The data are reported in Table 10. The anomalous room temperature behavior of this material which resulted in a 0.2% offset yield strength in excess of the apparent ultimate strength is being investigated and additional specimens are being prepared for testing. The material's excellent room temperature notch ductility is indicated by a notched to unnotched tensile strength ratio of 1.7:1.

Creep testing of round bar test specimens has been delayed until thoriated tungsten inserts for the round bar grips are received⁽²⁾. The promised shipping date is July 15.

D. PHASE IDENTIFICATION AND MORPHOLOGY

Phase identification and morphology studies were continued in an attempt to develop a better understanding of the effects of dispersed phase composition, morphology, and stability on the creep behavior of the experimental alloys being developed under this contract. A number of experimental techniques, which will be discussed briefly, are being used to obtain

TABLE 10 - Mechanical Properties of NASV-11
(Ta-9W-1.5Re-1Hf-0.015C-0.015N)

Test Temperature (°F)	Yield Strength			Ultimate Tensile Strength (psi)	% Elongation		% Reduction in Area
	Upper (psi)	Lower (psi)	0.2% Offset (psi)		Uniform	Total	
R.T. ^(a)	145,600	134,400	145,800	140,800	13.4	32.1	77.3
2000 ^(b)	--	--	57,500	93,900	--	23.1	69.1
2400 ^(b)	--	--	43,700	62,400	--	24.2	75.6
2800 ^(b)	--	--	30,800	40,100	--	40.3	63.5
R.T. (Notched-K _t = 3) ^(b)	--	--	--	244,000	--	--	7.2

(a) Strain rate 0.005 in./in./min. through 0.6% yield and then 0.05 in./in./min. for balance of test.

(b) Strain rate of 0.05 in./in./min. throughout test.

the desired information. Each has certain advantages and limitations and yields specific information not readily obtained by other techniques. One of these techniques requires the extraction of the dispersed phase from the matrix. The bulk extracted residue is obtained by dissolving the matrix of the sample in a solution which consists of 10 grams tartaric acid-10 ml bromine-90 ml methanol⁽³⁾. Platinum wire is wrapped around the sample being dissolved to catalyze the reaction. The resulting residue is then carefully washed with methanol and dried in vacuo. Identification of the phases comprising the residues is made by x-ray analysis, using the standard Debye-Scherrer technique. A semi-quantitative analysis of the metallic components of the compound(s) is obtained utilizing x-ray fluorescence. A Siemens Crystalloflex IV x-ray diffraction unit is used for the x-ray diffraction and fluorescence analysis.

The residue is also studied by electron microscopy. This is accomplished by ultrasonically dispersing the residue in amyl acetate and spreading a drop of the dispersion between two clean glass slides. Replicas containing the extracted and dispersed particles are then made by a two-stage carbon replica process quite similar to that developed by Bradley⁽⁴⁾. Transmission electron microscopy and selected area electron diffraction of the phases dispersed on these replicas are used to better define their size, shape, and structure. The diffraction pattern obtained from a thin layer of vapor deposited aluminum is used as the reference standard. All electron microscopy is done using the JEM-6A electron microscope.

The dispersed second phases are also studied in situ and thus a mounted and metallographically prepared sample of the material to be studied is required. Satisfactory metallographic preparation of the alloys developed under this contract has presented some difficulty in that the metallographic techniques used initially preferentially etched out the dispersed phases, particularly the nitrides. An intensive investigation was required to develop suitable polishing and etching techniques which would reproducibly retain the various dispersed phases in the alloy matrix. Two different metallographic preparation methods were developed; one for the carbide containing alloys and one for the nitride containing alloys.

These processes essentially consisted of mechanical polishing, acid polishing, and chemical etching, and mechanical polishing and cathodic vacuum etching respectively. Detailed procedures are in Appendix II. Alloys containing both carbon and nitrogen can be prepared by the procedure developed for carbide containing alloys, if the nitrogen is combined in the form of carbo-nitrides rather than as nitrides. Otherwise the procedure for nitride containing alloys must be used.

Once a satisfactory metallographic preparation is obtained, the sample can then be studied by optical and electron microscopy. In optical microscopy oblique lighting is used to confirm the presence or absence of the precipitates. Surface replicas are obtained using a two-stage carbon technique. These surface replicas are shadowed with chromium. Polystyrene spheres are used for referencing elevation and/or depression, by adding them to the replica prior to shadowing.

Transmission electron microscopy and selected area electron diffraction of extraction replicas, and electron beam micro-probe analysis of samples are two additional techniques being used. An extraction replica process capable of consistently producing high quality results is still being developed. Thus far, only one sample has been studied by means of the electron beam microprobe.

The phase identification and morphology work to date has been done to develop the techniques and procedures which will be required for the detailed morphology and phase identification investigation of the three 4-inch diameter ingot compositions. Thus some of the compositions reported on were only studied briefly, using one or two of the available techniques. The results obtained during this period will be discussed under the following compositional headings: Ta-W-Hf-C system, Ta-W-Zr-N system, and the Ta-W-Hf-Zr-C-N system. The x-ray diffraction data discussed in this report are included in Appendix III.

a. Ta-W-Hf-C System — Samples of Ta-9W-1Hf-0.025C (NASV-9) were studied

in the as-rolled condition, in the annealed condition (1 hour at temperatures of 1200, 1400, 1600, 1800, and 2000°C), and in the annealed and aged condition (506 hours aging at 1315°C after a 1-hour anneal at temperatures of 1600, 1800, and 2000°C). The chemically extracted dispersed phases in each of these samples were examined by means of standard x-ray diffraction techniques. The results are listed in Table 11. A HCP phase, which has been identified as the dimetal carbide of tantalum, was essentially the only phase present in any of the samples regardless of their mechanical-thermal history.

Lattice parameters, a_0 and c_0 , of the dimetal carbide ranged from 3.10 to 3.11 and from 4.92 to 4.96 Å respectively. These values compare closely with the values of $a_0 = 3.106$ Å and $c_0 = 4.945$ Å reported for Ta_2C ^(5,6). Only minor substitution of W and/or Hf for Ta occurs in the Ta_2C compound^(5,6). Appreciable line broadening was observed in the samples annealed for 1 hour at 1800°C (3270°F) and for 1 hour at 2000°C (3630°F). This line broadening was probably due to a very small particle size, although strain produces similar results. Minor amounts of the monoclinic form of HfO_2 were also present in a number of the samples, including all three of the annealed and aged samples. It is also undoubtedly present in the remaining samples, but in undetectable quantities. A very minor amount of an unidentified phase was present in the three annealed and aged samples (see the x-ray data in Appendix III). The FCC monocarbide of hafnium was not observed in any of the samples.

Two creep specimens of composition NASV-9 were also studied in detail. The first specimen (NASV-9T-2C) had been annealed for 1 hour at 1650°C (3000°F) and tested for 210 hours at 1315°C (2400°F) under a stress of 15,000 psi at 10^{-8} torr. The second specimen (NASV-9B-5C) had been annealed for 1 hour at 1800°C (3270°F) and tested for 500 hours under identical conditions of temperature, stress, and test pressure. As previously reported, x-ray diffraction analysis of the chemically extracted residues indicated the existence of the HCP dimetal carbide of tantalum having lattice parameters, a_0 and c_0 , of 3.11 Å and 4.96 Å respectively, in both the specimens as well as trace amounts of HfO_2 .

TABLE 11 - Results of X-ray Diffraction Analyses on Samples of Composition NASV-9^(a). (Ta-9W-1Hf-0.025C)

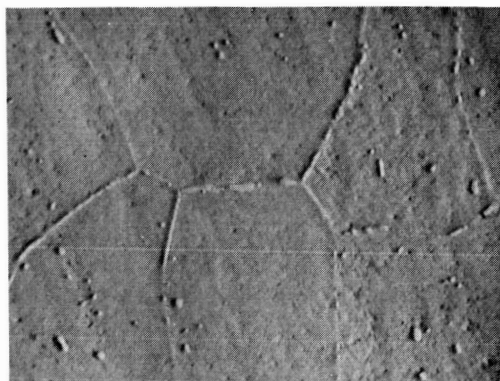
Condition	Phases Identified	Comments
As-Rolled (0.04")	$Ta_2C(s)(a_o = 3.11 \text{ \AA}, c_o = 4.95 \text{ \AA})$	HfO_2 (VW)
As-Rolled + 1 hr at 1200°C/2190°F	$Ta_2C(s)(a_o = 3.11 \text{ \AA}, c_o = 4.95 \text{ \AA})$	Extra line at 2.95 (VW) HfO_2 (VW)
+ 1 hr at 1400°C/2550°F	$Ta_2C(s)(a_o = 3.11 \text{ \AA}, c_o = 4.94 \text{ \AA})$	HfO_2 (VW)
+ 1 hr at 1600°C/2910°F	$Ta_2C(s)(a_o = 3.11 \text{ \AA}, c_o = 4.96 \text{ \AA})$	
+ 1 hr at 1800°C/3270°F	$Ta_2C(s)(a_o = 3.10 \text{ \AA}, c_o = 4.92 \text{ \AA})$	Lines are broad and diffuse
+ 1 hr at 2000°C/3630°F	$Ta_2C(s)(a_o = 3.10 \text{ \AA}, c_o = 4.92 \text{ \AA})$	Lines are broad and diffuse
As-Rolled + 1 hr at 1600°C/2910°F + 506 hrs. at 1315°C/2400°F	$Ta_2C(s)(a_o = 3.11 \text{ \AA}, c_o = 4.95 \text{ \AA})$	HfO_2 (W) Unidentified Phase
1 hr at 1800°C/3270°F + 506 hrs. at 1315°C/2400°F	$Ta_2C(s)(a_o = 3.11 \text{ \AA}, c_o = 4.95 \text{ \AA})$	HfO_2 Unidentified Phase
1 hr at 2000°C/3630°F + 506 hrs. at 1315°C/2400°F	$Ta_2C(s)(a_o = 3.11 \text{ \AA}, c_o = 4.95 \text{ \AA})$	HfO_2 Unidentified Phase Extra line at 1.88 (VW)

(a) Material rolled to 0.06 inch thickness, annealed for 1 hour at 1700°C (3090°F), radiation cooled, rolled to 0.04 inch thickness, and given the heat treatment specified.

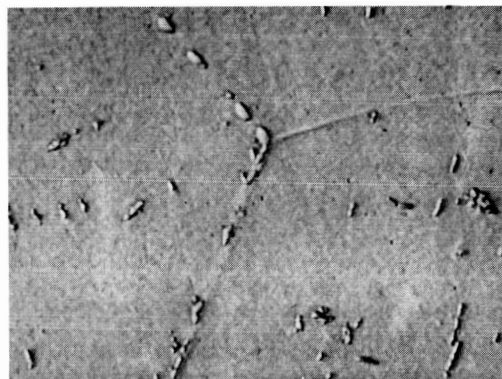
The microstructure of the gage lengths of specimens NASV-9T-2C and NASV-9B-5C is illustrated in Figures 5(a) and (b) respectively. The difference in grain size between the two specimens is due to the difference in the pre-test annealing temperature (1650°C versus 1800°C). Examination of surface replicas, made of the gage length of the two specimens using the two stage carbon technique, indicated the presence of a sub-micron dispersion of the dimetal carbide in specimen annealed at 1800°C (Figure 5c) which was not observed in the specimen annealed at 1650°C prior to test.

Several other alloys belonging to the Ta-W-Hf-C system were studied, but in less detail than NASV-9. These alloys consisted of compositions NAS-21 (Ta-8.6W-0.53Hf-0.02C), NAS-27 (Ta-4.6W-1.56Hf-0.05C), and NASV-2 (Ta-8W-2Hf-0.05C). The identity of the phases present in a single creep specimen of each of three compositions was determined by x-ray diffraction analysis of the extracted residues. The HCP dimetal carbide, $(\text{Ta,W,Hf})_2\text{C}$, and a minor amount of the FCC monocarbide, $(\text{Hf,Ta})\text{C}_{1-x}$, were observed to exist in specimen NASV-2-1C, which was annealed for 1 hour at 1650°C (3000°F) and tested in creep for 96.4 hours at 1315°C (2400°F) under an applied stress of 14,095 psi. The expanded lattice ($a_o = 3.12 \text{ \AA}$ and $c_o = 4.98 \text{ \AA}$) of the dimetal carbide is indicative of the substitution of some Hf for Ta since W substitution would tend to shrink the lattice. The observed lattice parameter value of the monocarbide of 4.60 \AA for $\text{HfC}_{1.0}^{(6)}$ is indicative of a compound of $(\text{Hf,Ta})\text{C}_{1-x}$ and agrees with the values reported by Ammon and Begley for the monocarbide present in T-222⁽⁷⁾. It should be noted that while both compositions NASV-2 and NASV-9 have the same Hf/C ratio, composition NASV-2 has twice as much of each element as does composition NASV-9.

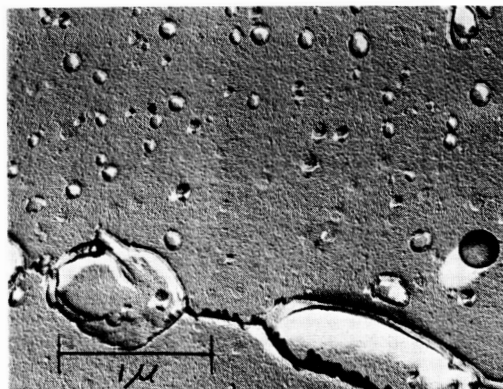
The HCP dimetal carbide, $(\text{Ta,W,Hf})_2\text{C}_{1-x}$, ($a_o = 3.11 \text{ \AA}$ and $c_o = 4.95 \text{ \AA}$), and very minor amounts of the FCC monocarbide, $(\text{Hf,Ta})\text{C}_{1-x}$, ($a_o = 4.58 \text{ \AA}$) and HfO_2 were observed in the residue chemically extracted from specimen NAS-27-1C. Severe line broadening was observed in the back reflection lines of the dimetal carbide, indicating a variable composition, possibly in substitution of W and/or Hf for Ta or in the C/Ta ratio. This specimen was given



- (a) NASV-9T-2C Annealed
1 hr/1650°C (3000°F)
then tested for 210 hrs at
1315°C (2400°F) and
15,000 psi at 10^{-8} Torr.
Optical micrograph (oblique
light) 1500X.



- (b) NASV-9B-5C Annealed
1 hr/1800°C (3270°F) then
tested for 500 hrs at 1315°C
(2400°F) and 1500 psi at
 10^{-8} Torr.
Optical micrograph
(oblique light) 1500X.



- (c) NASV-9B-5C. See figure
5b (above) Electron
Micrograph 20,000X.

FIGURE 5 - Optical and Electron Micrographs of Creep Specimens of Composition NASV-9 (Ta-9W-1Hf-0.025C). Precipitates are tantalum dimetal carbides.

the standard pre-test anneal of 1 hour at 1650°C (3000°F) and tested in creep for 76 hours at 1315°C (2400°F) under an applied stress of 10,000 psi. Composition NAS-27 has a lower Hf/C ratio than does composition NASV-9, but it does have a higher Hf and C concentration.

Only the HCP dimetal carbide, $(\text{Ta,W,Hf})_2\text{C}_{1-x}$, having lattice parameters of $a_o = 3.11 \text{ \AA}$ and $c_o = 4.95 \text{ \AA}$, was detected in the residue extracted from specimen NAS-21-1C. This specimen was also given the standard anneal and tested in creep for 96.1 hours at 1315°C (2400°F) under a stress of 15,070 psi. Composition NAS-21 has a lower Hf/C ratio than does composition NASV-9, and both Hf and C are present in small amounts.

As would be expected, the amount of Hf and/or C is more significant than the ratio of Hf to C in determining the precipitating phase (i.e., FCC monocarbide and/or HCP dimetal carbide). For the basic Ta-W-Hf-C system, the boundary between the two phase BCC solid solution-dimetal carbide region and the three phase BCC solid solution-dimetal carbide-monocarbide region for the 1315°C (2400°F) isotherm, in this study, is shown in Figure 6.

A T-111 (Ta-8W-2Hf) creep specimen (discussed in Reference 1), which was contaminated during a 172-hour creep test in an oil diffusion pumped system operating at 10^{-6} torr, was extensively studied. This study was made to determine the cause of the four-fold reduction in its creep rate compared to that of similar T-111 specimens which had been tested at 1370°C/2500°F in a hydrocarbon free sputter ion pumped system operating at 10^{-8} to 10^{-9} torr. Chemical analysis⁽¹⁾ of the specimen after creep testing had indicated a net increase of 235 ppm carbon to 260 ppm and of 275 ppm oxygen to 290 ppm, essentially making its composition Ta-8W-2Hf-0.026C-0.029O. Analysis of the extracted residue by standard x-ray diffraction techniques indicated the presence of a FCC phase having a lattice parameter a_o of 4.60 Å. This phase was assumed to be the monocarbide $(\text{Hf,Ta,W})\text{C}_{1-x}$, contaminated to some degree with oxygen. A minor amount of HfO_2 was also present. Surprisingly the HCP dimetal carbide phase, which should be expected to be present in this sample was not found. A comparison of the phases existing in this specimen with those existing in specimen

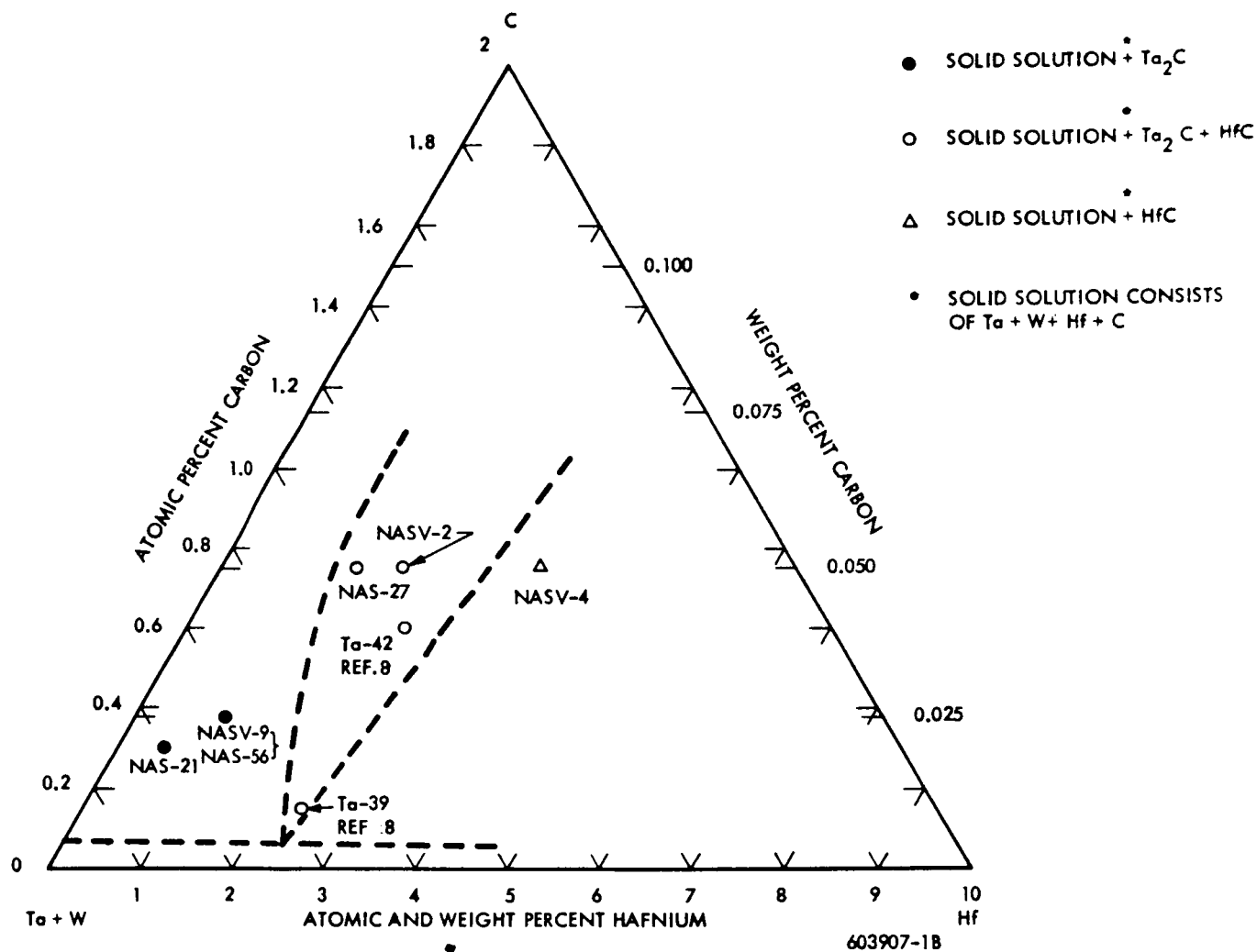


FIGURE 6 - 1315°C (2400°F) Isotherm of Tantalum Corner of (Ta,W)-Hf-C Pseudo Ternary System

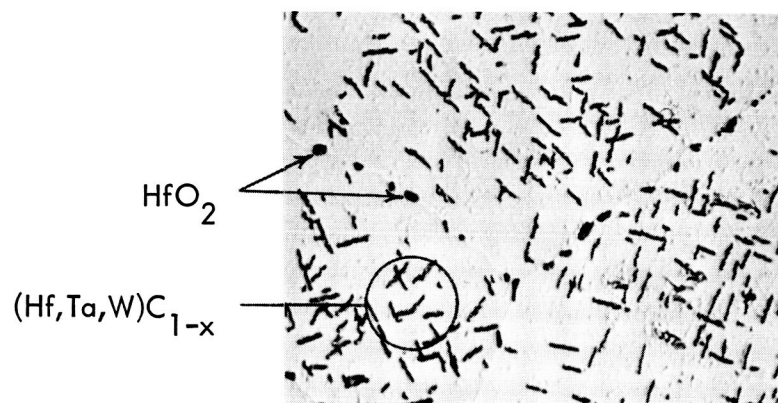
NASV-2-1C, and also with data reported elsewhere⁽⁸⁾, suggests that the presence of the significant amount of oxygen preferentially stabilizes the FCC monocarbide phase.

The microstructure of the contaminated creep specimen gage length is shown in Figure 7a. The globular grain boundary precipitates are the monoclinic form of HfO_2 and the platelets in the matrix were assumed to be the monocarbide. The platelets of the monocarbide were very thin, transparent to the electron beam, and badly faulted (Figure 7b). The HfO_2 particles were non-transparent and were often regularly shaped. As the precipitate shown in Figures 7a and b are too large, and present in an insufficient amount to be effective inhibitors of creep, the reduced creep rate was assumed to be due to a much finer dispersoid. Such a dispersoid consisting of particles about 0.03μ in diameter was indeed observed (Figure 7c) by means of electron microscopy. Positive identification of this dispersoid has not yet been made.

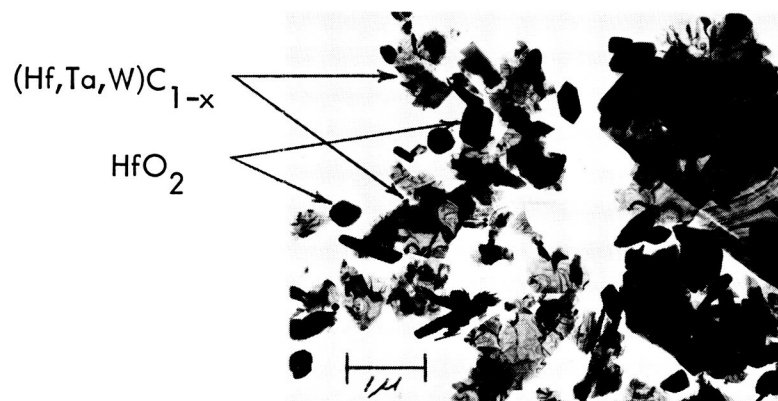
The next composition studied was NAS-56 (Ta-8W-1Re-0.7Hf-0.025C) which is identical to composition NASV-9 except that 1% Re is substituted for 1% W. The effect of the Re substitution on phase identity and morphology was determined by a thorough examination of two creep specimens, NAS-56-1C and NAS-56-2C. The first specimen was annealed for 1 hour at 1650°C (3000°F) and tested in creep for 211 hours at 1315°C (2400°F) under an applied stress of 12,690 psi. The second was similarly annealed and tested in creep for 230 hours at 1315°C (2400°F) under a stress of 15,000 psi.

X-ray diffraction analysis of the dispersed phases extracted from the gage section of each specimen indicated that except for a trace of HfO_2 in specimen NAS-56-1C, the residues consisted entirely of the HCP dimetal carbide, $(\text{Ta,W,Hf})_2\text{C}_{1-x}$, similar to the residues extracted from composition NASV-9. Its lattice parameters were $a_o = 3.11 \text{ \AA}$ and $c_o = 4.95 \text{ \AA}$.

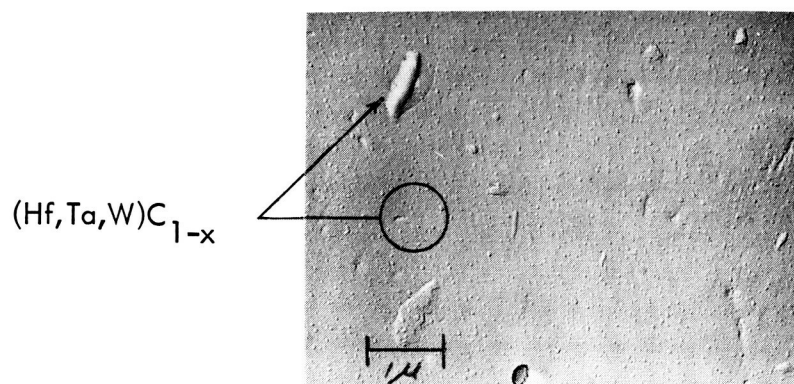
The microstructure of the two specimens' gage lengths is shown in Figures 8 a and b. Note the grain boundary precipitates are much more massive and continuous than those present



(a) Optical Micrograph
1,500X



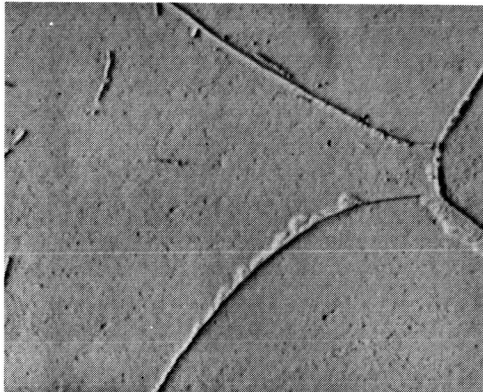
(b) Transmission
Electron Micrograph
of Extracted Residue
10,000X



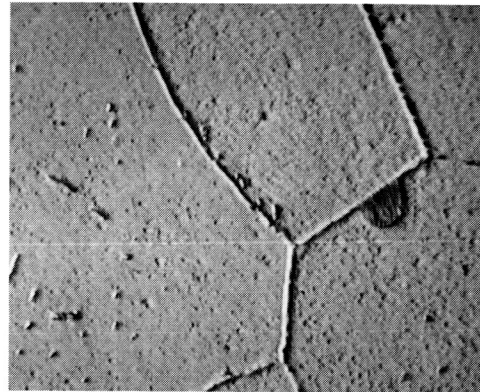
(c) Electron Micrograph
10,000X

FIGURE 7 - Optical and Electron Micrographs of T-111 (Ta-8W-2Hf) Creep Specimen Contaminated* During Testing for 172 hrs at 1370°C (2500°F) at 10⁻⁶ Torr.

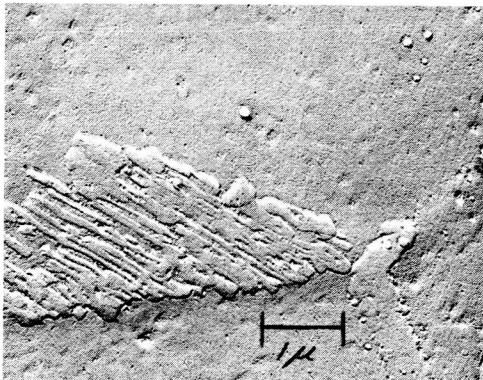
*With 260 ppm C and 290 ppm O).



(a) NAS-56-1C
Optical Micrograph
(Oblique Light)
1,500X

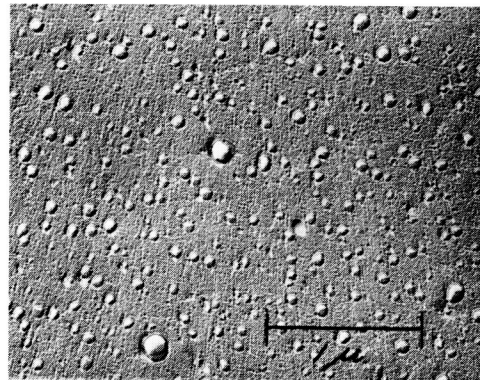


(b) NAS-56-2C
Optical Micrograph
(Oblique Light)
1,500X



(c) Electron Micrograph
(NAS-56-1C)

10,000X



(d) Electron Micrograph
(NAS-56-1C)

20,000X

FIGURE 8 - Optical and Electron Micrographs of Creep Specimens of Composition NAS-56 (Ta-8W-1Re-0.7 Hf-0.025C). Specimen NAS-56-1C was annealed for 1 hr at 1650°C (3000°F) and tested for 211 hrs at 1315°C (2400°F) under 12,690 psi at 10^{-8} torr. Specimen NAS-56-2C was similarly annealed and tested for 230 hrs at 1315°C (2400°F) under 15,000 psi at 10^{-8} torr. Precipitates are tantalum dimetal carbides.

in the NASV-9 specimens (Figures 5a and b). However, they did not adversely effect the creep behavior nor the room temperature ductility of the alloy. Surface replicas of the two NAS-56 specimens indicated that the grain boundary precipitates actually were composed of a number of parallel dimetal carbide platelets (Figure 10c). They also indicated the presence of a sub-micron form of the dimetal carbide (Figure 10d) similar to that found in specimen NASV-9B-5C, but which was slightly smaller and more evenly dispersed. The residues extracted from these two specimens will be examined by means of electron microscopy to better determine the size and shape of the two different forms.

It is evident that while the Re did not effect the crystallographic structure of the dispersed phase, it did affect its morphology. No indication of Re has been found in the extracted residues by means of x-ray fluorescence techniques. Possibly through the resulting morphology changes, the Re addition resulted in a two-fold decrease in the minimum creep rate from that measured in a specimen of composition NASV-9 given the same anneal and tested under the identical conditions of temperature and stress (i.e., 0.0034%/hour for specimen NAS-56-2C versus 0.0070%/hour for specimen NASV-9B-5C). The smaller, more evenly dispersed matrix precipitate is possibly responsible for this decreased creep rate rather than the solid solution strengthening effect of the Re addition.

The effect of the addition of Zr on the resulting dispersed phase(s) was determined by examining a creep specimen of composition NASV-4 (Ta-8W-2.6Hf-0.4Zr-0.05C). This specimen, NASV-4-2C, had been annealed for 1 hour at 1650°C (3000°F) and tested for 70 hours at 1315°C (2400°F) under an applied stress of 14,000 psi. An x-ray analysis of the residue extracted from the specimen's gage length indicated that it was composed of three distinct FCC phases, having the lattice parameter, a_0 , of 4.58 Å, 4.61 Å, and 5.10 Å, respectively. The first two phases were present in moderate amounts and were believed to be the monocarbides of Hf and Zr. Carbon deficiencies, substitution of Ta for the Hf and Zr, and/or the presence of residual oxygen and/or nitrogen are probably responsible for the reduction of the lattice parameters from the reported values of 4.641 Å for HfC⁽⁶⁾ and 4.702 Å for ZrC⁽⁶⁾.

X-ray fluorescence analysis will be made on the extracted residue to determine the relative amounts of Hf, Ta, and Zr present. Only a minor amount of the third phase was present, and it has been tentatively identified as a cubic form of ZrO_2 . No evidence of the HCP dimetal carbide was observed. Evidently 3.4 a/o Hf plus Zr was sufficient to stabilize the FCC monocarbide phase. Thus, assuming Zr and Hf behave identically the boundary between the three phase matrix-dimetal carbide-monocarbide region and the two phase matrix-monocarbide region must lie between the 2% Hf-0.05% C of composition NASV-2 and to 3.4 a/o Hf plus Zr-0.05% C of composition NASV-4.

The creep resistance of composition of NASV-4 was relatively poor. This poor resistance to creep can in part be attributed to the presence of a much greater than stoichiometric amount of reactive metal (Hf plus Zr)⁽¹⁾.

b. Ta-W-Zr-N System — The basic Ta-W-Zr-N system was studied in less detail primarily to determine the size, shape, and morphology of the zirconium-nitrogen phases prior to working with more complex compositions combining both of the basic Ta-W-Hf-C and Ta-W-Zr-N systems. X-ray diffraction analyses were made on the residue extracted from two samples of composition NAS-42 (Ta-5.3W-1.56Re-0.65Mo-0.52Zr-0.08N). One sample had been annealed for 1 hour at 1650°C (3000°F). The second had been annealed for 1 hour at 2000°C (3630°F) and aged for 500 hours at 1250°C (2280°F). The FCC phase, assumed to be ZrN , was the only major phase detected in either residue. Its lattice parameter was 4.57 Å, indicating a N/Zr atom ratio somewhat less than 1.0⁽⁹⁾. A minor amount of the FCC phase, having a lattice parameter, a_o , of 5.10 Å, was also detected. This phase tentatively identified as a cubic ZrO_2 was previously found in creep specimen NASV-4-2C.

Electron micrographic examination of the extracted residues shows that the major FCC phase, ZrN , was present in the form of very small, extremely thin platelets approximately 300 to 500 Å thick. Those from the annealed sample were quite regularly shaped and ranged in size up to 1/2 micron, while those from the annealed and aged material appeared to be somewhat less regularly shaped and ranged in size up to 1 micron.

c. Ta-W-Hf-Zr-C-N — The first of two complex alloys, combining the basic Ta-W-Hf-C and Ta-W-Zr-N systems, studied was composition NASV-7 (Ta-5.7W-1.56Re-0.7Mo-0.25Hf-0.13Zr-0.015C-0.015N). As with composition NASV-9, samples of this alloy were examined in the as-rolled condition, in the annealed condition (1 hour at 1200, 1400, 1600, 1800, and 2000°C), and in the annealed and aged condition (506 hour aging at 1315°C after a 1 hour anneal at temperatures of 1600, 1800, and 2000°C). The dispersed phases in each of these samples were extracted and examined by means of standard x-ray diffraction techniques. Results are listed in Table 12. A HCP phase assumed to be the dimetal carbide, $(Ta, W, Hf)_2 C_{1-x}$, was found in every sample except the one annealed at 2000°C (3630°F). Apparently, the solvus was exceeded at 2000°C and the composition was single phase. The presence of the dimetal carbide at the lower annealing temperature was expected. Its lattice parameter was essentially the same as that of the dimetal carbide present in composition NASV-9 (i.e., $a_o = 3.10$ to 3.11 \AA and $c_o = 4.92$ to 4.95 \AA for composition NASV-7 versus $a_o = 3.10$ to 3.11 \AA and $c_o = 4.92$ to 4.96 \AA for composition NASV-9). Again, the lattice parameters indicate only minor substitution of Hf and/or W for Ta. Besides the dimetal carbide, a minor amount of the monoclinic form of HfO_2 was present in many of the residues. A FCC phase corresponding to ZrN was not detected in the residues of any of the annealed samples, but was present in the residues of all three of the annealed and aged samples. The kinetics of precipitation of ZrN have been shown to be affected by the degree of supersaturation.⁽²⁾ The reported lattice parameter, a_o , of 4.60 \AA indicates a large nitrogen deficiency and/or the presence of ZrC. A small amount of BCC phase (a_o of 3.38 \AA and 3.74 \AA) present in the sample annealed for 1 hour at 2000°C (3630°F) were completely unanticipated and cannot presently be explained. Possibly they are complex metastable phases containing Zr, N, and C among other elements which decompose into the FCC mononitride phase during aging.

Two creep specimens of composition NASV-7 were also studied in considerable detail. The first specimen, NASV-7T-1C, was annealed for 1 hour at 1650°C (3000°F) and tested in creep for 190 hours at 1315°C (2400°F) under a stress of 15,000 psi. The second

TABLE 12 - Results of X-ray Diffraction Analyses on Samples of Composition
NASV-7^(a) (Ta-5.7W-1.56Re-0.7Mo-0.25Hf-0.13Zr-0.015C-0.015N)

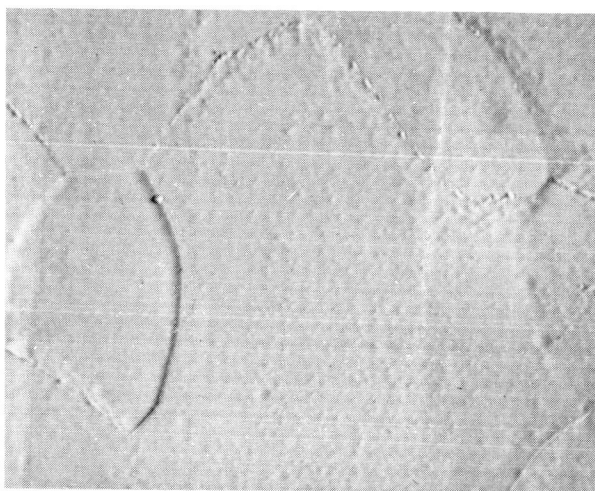
Condition	Phases Identified	Comments
As-Rolled (0.04")	Ta ₂ C(s) (a _o = 3.10 Å, c _o = 4.92 Å)	Extra line at 2.000 (VW). Lines are broad and diffuse.
As-Rolled		
+ 1 hr at 1200°C/2190°F	Ta ₂ C(s) (a _o = 3.10 Å, c _o = 4.94 Å)	
	HfO ₂	(VW)
+ 1 hr at 1400°C/2550°F	Ta ₂ C(s) (a _o = 3.11 Å, c _o = 4.95 Å)	Extra lines at 1.88 (VVW) and 1.72 (VW)
	HfO ₂	(VW)
	FCC (a _o = 5.10 Å)	Unidentified
+ 1 hr at 1600°C/2910°F	Ta ₂ C(s) (a _o = 3.10 Å, c _o = 4.92 Å)	
	HfO ₂	(VW)
	FCC (a _o = 5.10 Å)	Unidentified
+ 1 hr at 1800°C/3270°F	Ta ₂ C (a _o = 3.11 Å, c _o = 4.95 Å)	(M)
	Ta (a _o = 3.30 Å)	(M)
	BCC (a _o = 3.38 Å)	Unidentified (M)
+ 1 hr at 2000°C/3630°F	BCC (a _o = 3.40 Å)	Unidentified (M)
	BCC (a _o = 3.74 Å)	Unidentified (W)
As-Rolled		
+ 1 hr at 1600°C/2910°F + 506 hrs. at 1315°C/2400°F	Ta ₂ C (a _o = 3.11 Å, c _o = 4.95 Å)	(S) Extra line at 1.99 (VVW)
	ZrN (a _o = 4.60 Å)	(W)
	HfO ₂	(W)
	FCC (a _o = 5.10 Å)	Unidentified
+ 1 hr at 1800°C/3270°F + 506 hrs. at 1315°C/2400°F	Ta ₂ C (a _o = 3.11 Å, c _o = 4.94 Å)	(S) Extra lines at 1.98 (VVW) and 1.070 (VW)
	ZrN (a _o = 4.60 Å)	(W)
+ 1 hr at 2000°C/3630°F + 506 hrs. at 1315°C/2400°F	Ta ₂ C (a _o = 3.11 Å, c _o = 4.94 Å)	(S)
	ZrN (a _o = 4.60 Å)	(W)

(a) Material rolled to 0.06 inch thickness, annealed for 1 hour at 1700°C (3090°F), radiation cooled, rolled to 0.04 inch thickness, and given the heat treatment specified.

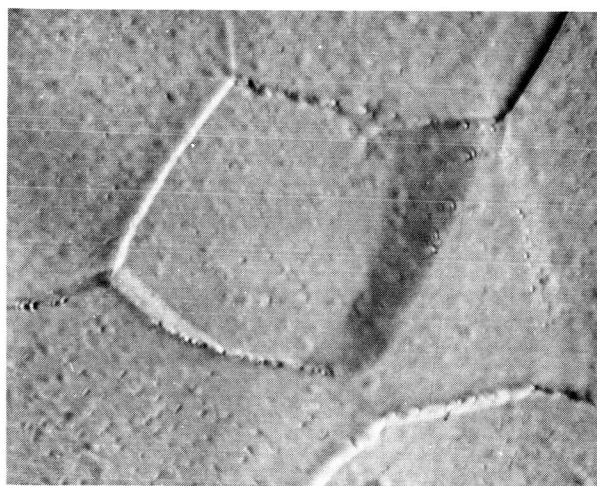
specimen, NASV-7T-5C, was annealed for 1 hour at 1800°C (3270°F) and tested in creep for 820 hours under the same conditions of temperature and stress. X-ray diffraction analyses made of the extracted residues of the two specimens were reported in the Fifth Quarterly Report. Results were essentially the same as for the previously discussed annealed and aged samples of composition NASV-7 (i. e., both specimens contained the HCP dimetal carbide phase having lattice parameters, a_o and c_o , of 3.11 Å and 4.94 Å respectively, and the FCC mononitride phase having a lattice parameter, a_o , of 4.58 Å.

The microstructures of the specimens' gage lengths (also discussed in the Fifth Quarterly Report) are shown in Figures 9a and b. Surface replicas of the same areas were carefully examined to better determine the size and shape of the included phases. Figure 10 illustrates the phases found in specimen NASV-7T-1C. The globular, often regularly shaped precipitates found in the grain boundaries, are particles of HfO_2 ; the thin, submicron platelets are the dimetal carbides; and the very small, thin, submicron platelets are the mononitrides. These latter two phases are approximately $1/2$ micron and less than $1/10$ micron in size respectively.

The phases as found in specimen NASV-7T-5C are illustrated in Figures 11a and b. Again the globular grain boundary precipitates are HfO_2 . The thin needles extending from the grain boundary are platelets of the dimetal carbide and the particles shown in Figure 11d are believed to be made up of very thin platelets of either the mononitride or a combination of both the mononitride and the dimetal carbide. The exact nature of the phases present in specimen NASV-7T-5C were more clearly defined by means of an electron microscopy study of the extracted residue. The results of this study are illustrated in Figures 12a and b, and are as expected from the previous work. The non-transparent particles are HfO_2 ; the 300 to 500 Å thick, badly faulted platelets are the dimetal carbide, and the 300 to 500 Å thick, comparatively fault-free platelets are the mononitride.



(a) NASV-7T-1C
Annealed for 1 hr/1650°C
(3000°F) then tested for
190 hrs at 1315°C (2400°F)
and 15,000 psi at 10⁻⁸ torr
(oblique light)
1500X



(b) NASV-7T-5C
Annealed for 1 hr/1800°C
(3270°F) then tested for 820
hrs at 1315°C (2400°F) and
15,000 psi at 10⁻⁸ torr
(oblique light)
1500X

FIGURE 9 - Optical Micrographs of Creep Specimens of
Composition NASV-7 (Ta-5.7W-1.56Re-0.7Mo-0.25Hf-
0.13-Zr-0.015C-0.015N)

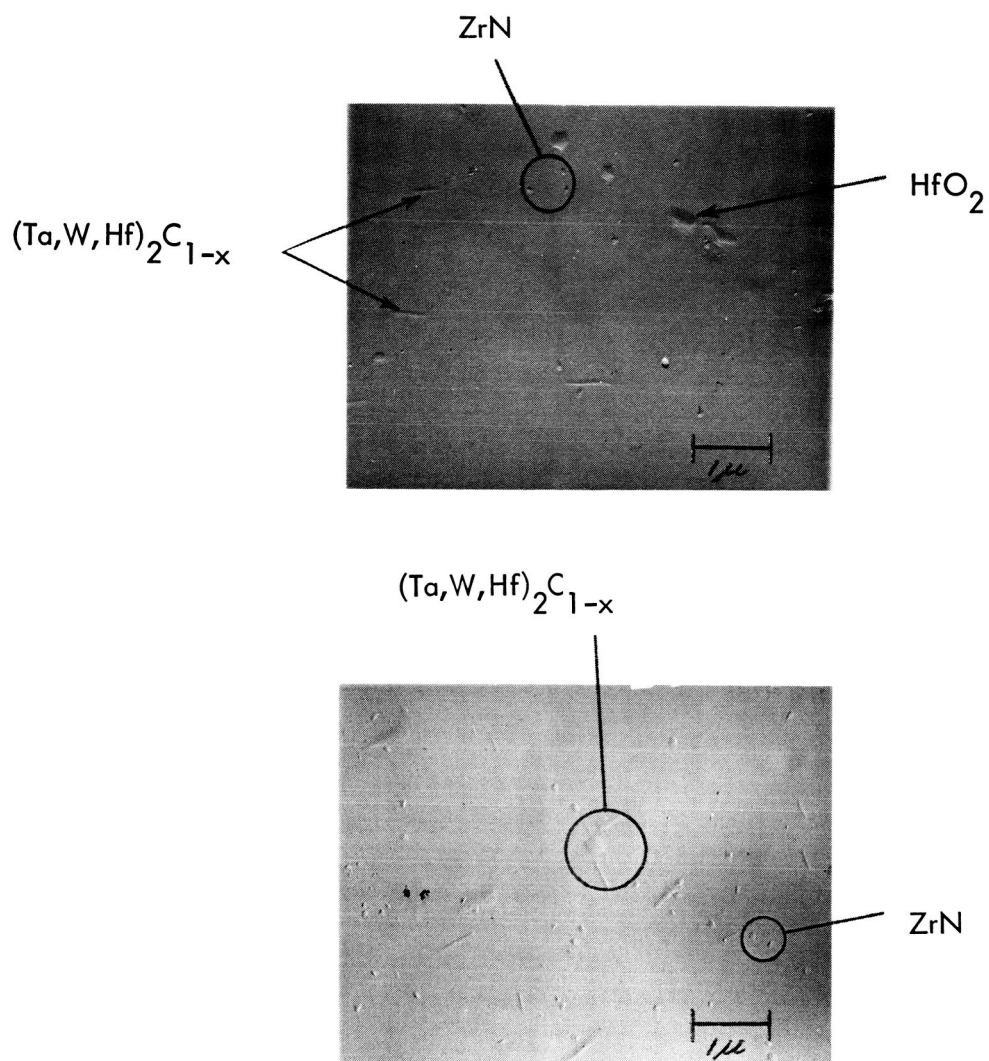


FIGURE 10 - Electron Micrographs of Creep Specimen T-1C of Composition NASV-7 (Ta-5.7W-1.56Re-0.7Mo-0.25Hf-0.13 Zr-0.015C-0.015N). Specimen was annealed for 1 hour at 1650°C (3000°F) and tested for 190 hours at 1315°C (2400°F) and 15,000 psi at 1×10^{-8} torr. 10,000X

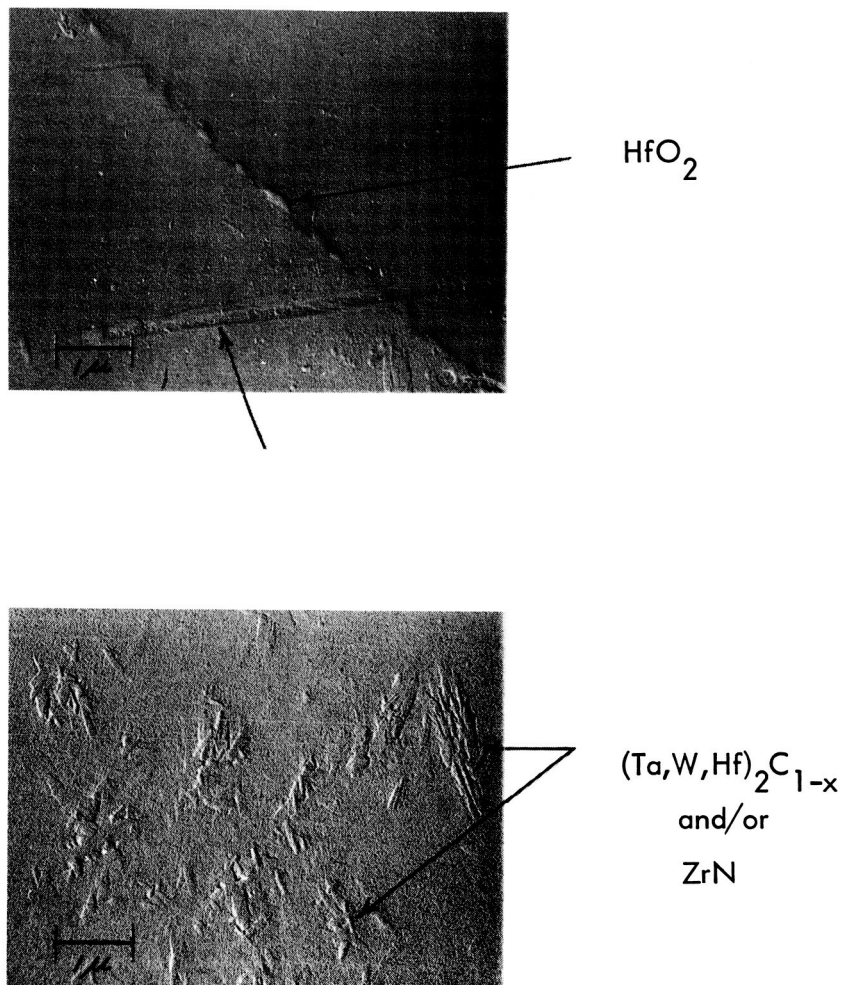


FIGURE 11 - Electron Micrographs of Creep Specimen T-5C, of Composition NASV-7 (Ta-5.7W-1.56Re-0.7Mo-0.25Hf-0.13Zr-0.015C-0.015N). Specimen was annealed for 1 hour at 1800°C (3270°F) and tested for 820 hours at 1315°C (2400°F) and 15,000 psi at 1×10^{-8} torr.
10,000X

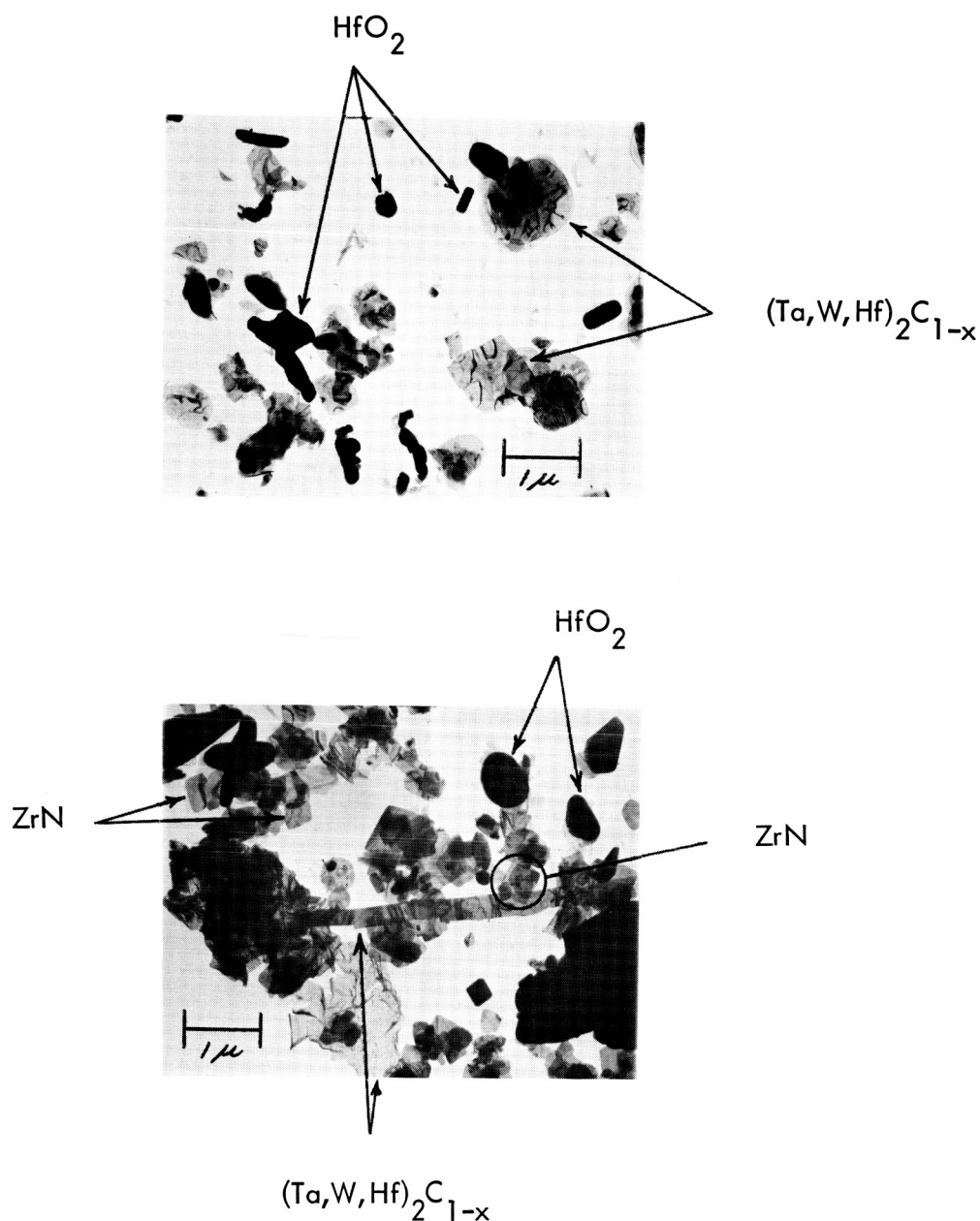


FIGURE 12 - Transmission Electron Micrographs of Precipitates Extracted From Creep Specimen T-5C, of Composition NASV-7 (Ta-5.7W-1.56Re-0.7Mo-0.25Hf-0.13Zr-0.015C-0.015N). Specimen was annealed for 1 hour at 1800°C (3270°F) and tested for 820 hours at 1315°C (2400°F) and 15,000 psi at 1×10^{-8} torr. 10,000X

Any differences in the morphology of the phases present in the two specimens can only be attributed to the difference in the annealing temperature prior to creep testing or to the difference in duration of the creep testing. The differences in the initial creep behavior of the two specimens (minimum creep rates of 0.003%/hour for specimen NASV-7T-1C and 0.001%/hour for specimen NASV-7T-5C) can be attributed in part to the grain size and in part to the resulting differences in the morphology of the phases present. It is interesting to note that the higher final annealing temperature of 1800°C (3270°F) resulted in a significantly reduced creep rate for composition NASV-7 just as it did for composition NASV-9.

An electron beam microanalysis was also made on the gage length of specimen NASV-7T-5C by Advanced Metals Research Corporation (AMR) in Burlington, Massachusetts. This analysis was made to determine the distribution of W, Mo, Re, Hf, and Zr across the thickness of the specimens gage length. The characteristic x-ray lines monitored were the $WL_{\alpha}(5)$, $MoL_{\alpha}(5)$, $HfL_{\alpha}(5)$, ZrL_{α} , and $TaL_{\alpha}(5)$. AMR reported the following:

"No differences in alloy chemistry are noted from the matrix to within 5 μ of the surface/edge. Surface rounding and the resolution of the electron beam become evident within 5 μ of the edge."

Furthermore, AMR reported the amount of the metallic elements present as determined by the microprobe to be Ta-5.8W-0.8Mo-1.53Re-0.49Hf-0.16Zr. These results, with the exception of Hf, are in excellent agreement with the nominal composition. Discreet analysis of the precipitates could not be made because of their very small size compared to the 1 micron diameter focused electron beam.

The second complex alloy and the last alloy studied was composition NASV-8 (Ta-5.7W-1.56Re-0.7Mo-0.75Hf-0.13Zr-0.015C-0.015N). This composition is identical to that of composition NASV-7 except that it contains 0.75% Hf instead of 0.25% Hf for a Hf/C atom ratio of approximately 4.8. A single creep specimen, NASV-8M-2C was examined in the usual manner. This specimen had been annealed for 1 hour at 1650°C (3000°F) and then tested in creep for 400 hours at 1315°C (2400°F) under a stress of 13,340 psi. X-ray

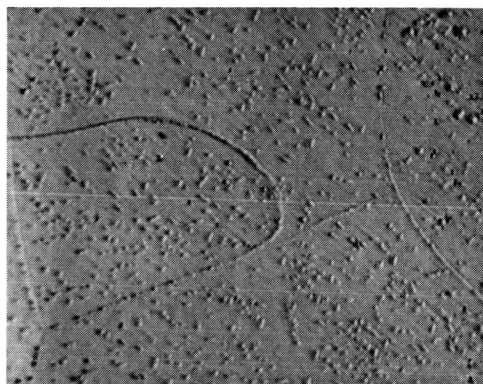
analysis of the extracted residue indicated the presence of two FCC phases. One of the phases comprised most of the extracted residue and had a lattice parameter, a_0 , of 4.59 \AA . This phase could be any of the monocarbides or mononitrides of Hf or Zr. However, it is most likely an isomorphous combination of two or more of these phases and will be tentatively identified as (Hf,Zr) (C,N). A trace of monoclinic HfO_2 and cubic ZrO_2 was also detected. The complete absence of the dimetal carbide would indicate that the three phase region of the proposed phase diagram has been in effect shifted towards the C or C and Ta+W ends of the diagram by the additional hafnium content.

The microstructure of the specimen's gage length is illustrated in Figures 13a, b, c, and d. The globular, regularly shaped particles, found in the grain boundaries are monoclinic HfO_2 and the platelet type precipitates are the (Hf,Zr) (C,N). Positive identification of the second FCC phase will be attempted by examining the extracted residue by means of electron microscopy and selected area electron diffraction techniques.

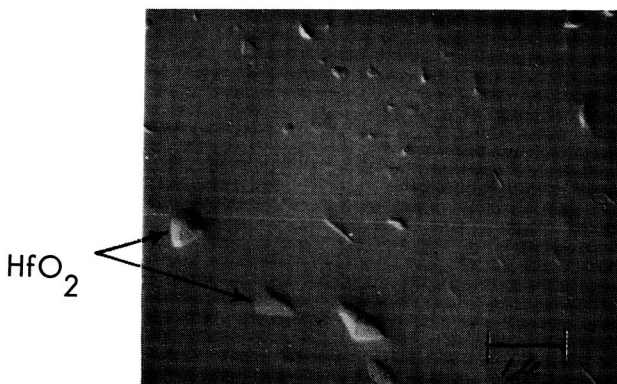
III. FUTURE WORK

During the next quarterly period it is planned to accomplish the following:

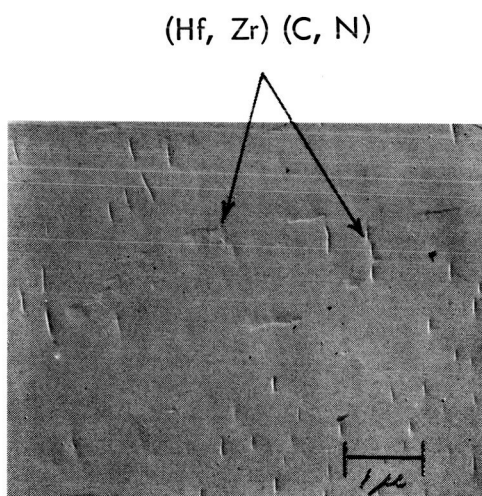
1. Complete melting of the optimized two-inch diameter ingot compositions.
2. Complete processing of the optimized compositions to 0.40-inch sheet, machine specimens from the sheet, and complete creep, fabricability, and tensile evaluations.
3. Complete processing of the first 4-inch diameter ingot composition, NASV-20, to 0.040-inch sheet, machine specimens from the sheet, and initiate creep, fabricability, and tensile evaluations.
4. Initiate phase identification and morphology investigations of dispersed phases in NASV-20 (Ta-8W-1Re-0.7Hf-0.025C).



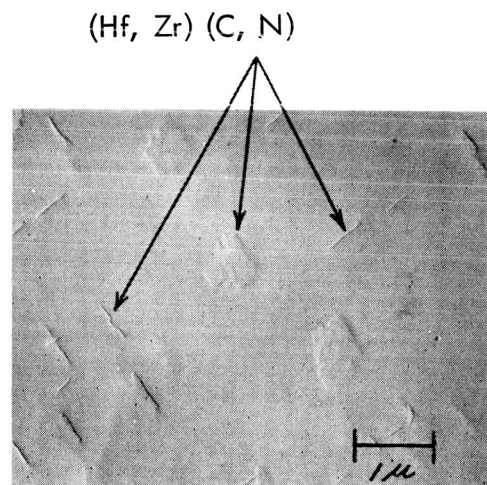
(a) Optical Micrograph
(Oblique Lighting)
1,500X



(b) Electron Micrograph
of Surface Replica
10,000X



(c) Electron Micrograph
of Surface Replica
10,000X



(d) Electron Micrograph
of Surface Replica
10,000X

FIGURE 13 - Optical and Electron Microscopy of Creep Specimen M-2C of Composition NASV-8 (Ta-5.7W-1.56Re-0.7Mo-0.75Hf-0.13Zr-0.015C-0.015N). Specimen was annealed for 1 hour at 1650°C (3000°F) and tested for 400 hours at 1315°C (2400°F) and 13,340 psi at 1×10^{-8} torr.

IV. REFERENCES

1. R. W. Buckman R. T. Begley, "Development of Dispersion Strengthened Tantalum Base Alloys", Final Technical Report, Phase I, WANL-PR-(Q)-004, Contract NAS 3-2542.
2. R. W. Buckman, "Development of Dispersion Strengthened Tantalum Base Alloy", 5th Quarterly Report, WANL-PR-(Q)-006.
3. R. T. Begley, W. N. Platte, R. L. Ammon, A. I. Lewis, "Development of Niobium-Base Alloys", WADC-TR-57-344, Part V, January 1961.
4. D. E. Bradley, "A High-Resolution Evaporated-Carbon Replica Technique for the Electron Microscope", Journal of the Institute of Metals, Vol. 83, pp. 35-38, 1954-1955.
5. E. Rudy and H. Nowotny, "Untersuchen in System Hafnium-Tantal-Kohlenstoff", Mh. Chemie, 94 pp. 507-517, 1963.
6. LAMS-2674 (Part I), "A Critical Review of Refractories - Part I - Selected Properties of Group 4A, 5A, and 6A Carbides", by E. K. Storms, 1962.
7. R. L. Ammon and R. T. Begley, "Pilot Production and Evaluation of Tantalum Alloy Sheet", Summary Phase Report, Part II, WANL-PR-M-009, July 1, 1964, Prepared under Navy Contract N600(19)-59762.
8. R. L. Ammon and A. M. Filippi, "Pilot Production and Evaluation of Tantalum Alloy Sheet", Quarterly Report No. 9, WANL-PR-M-011.
9. LAMS-2674 (Part II), "A Critical Review of Refractories - Part II - Selected Properties of Group 4A, 5A, and 6A Nitrides", by E. K. Storms, 1962.

APPENDIX I

Compositions of alloys discussed in this report are listed below:

<u>Heat Number</u>	<u>Composition Weight Percent</u>
<u>Consumable Electrode Melted, 2-Inch Diameter</u>	
NASV-2	Ta-8W-2Hf-0.05C
NASV-4	Ta-8W-2.7Hf-0.4Zr-0.05C
NASV-7	Ta-5.7W-1.56Re-0.7Mo-0.25Hf-0.13Zr-0.015N-0.015C
NASV-8	Ta-5.7W-1/56Re-0.7Mo-0.75Hf-0.13Zr-0.015N-0.015C
NASV-9	Ta-9W-1Hf-0.025C
NASV-10	Ta-7.1W-1.56Re-0.25Hf-0.12Zr-0.03N
NASV-11	Ta-9W-1.5Re-1Hf-0.015C-0.015N
NASV-12	Ta-7.5W-1.5Re-0.5Hf-0.015C-0.015N
NASV-13	Ta-6.5W-2.5Re-0.3Hf-0.01C-0.01N
NASV-14	Ta-4W-1Mo-2Re-0.3Zr-0.015C-0.015N
NASV-15	Ta-9W-1.5Re-1Hf-0.06N
NASV-16	Ta-9.5W-0.5Re-0.25Zr-0.02C-0.01N
NASV-17	Ta-4W-3Re-0.75Hf-0.01C-0.02N
NASV-18	Ta-5W-1Re-0.3Zr-0.025N Ta-6W-1Mo-1Re-0.7Hf-0.025C
NASV-20(4" Dia.)	Ta-8W-1Re-0.7Hf-0.025C
<u>Non-Consumable Electrode Melted</u>	
NAS-36	Ta-5.7W-1.56Re-0.7Mo-0.25Hf-0.13Zr-0.015C-0.015N
NAS-21	Ta-8.6W-0.54Hf-0.02C
NAS-27	Ta-4.6W-1.5Hf-0.05C
NAS-42	Ta-5.3W-1.58Re-0.65Mo-0.52Zr-0.08N
NAS-56,57	Ta-8W-1Re-0.7Hf-0.025C

APPENDIX II

Metallographic Procedures

STANDARD PROCESS OUTLINE FOR THE METALLOGRAPHIC PREPARATION OF TANTALUM BASE ALLOYS CONTAINING CARBIDES

The standard method of metallographically preparing tantalum base alloys containing carbides for light and electron microscopy shall consist of mechanical polishing and etching, per the following:

Mechanical Polishing: In mechanical polishing the specimen shall be ground in the usual manner on 240, 400, and 600 grit silicon carbide papers. The scratches from the last paper shall then be removed by polishing with 30, 15, and 6 micron diamond abrasives for short times on a hard-finish cloth (i. e. , unbleached muslin, Premier suede drill cloth, etc.). The mechanical polish shall be continued with very light pressure on a short-pile cloth (i. e. , Buehler Microcloth) charged with a thick slurry of Linde B alumina abrasive and water. Finally, the specimen shall be acid polished, by addition of a 2 to 4% chromic acid solution to the polishing cloth, while still charged with the Linde B abrasive.

Etching: The specimen shall be etched in a solution consisting of 1 part of concentrated nitric acid, 1 part of 48% hydrofluoric acid, and 2 parts of glycerine. The etching time shall be kept to a minimum required to fully reveal the microstructure.

STANDARD PROCESS OUTLINE FOR THE METALLOGRAPHIC PREPARATION OF TANTALUM BASE ALLOYS CONTAINING NITRIDES

The standard method of metallographically preparing specimens of tantalum base alloys containing nitrides for light and electron microscopy shall consist of mechanical polishing and cathodic vacuum etching, per the following:

Mechanical Polishing: In mechanical polishing the specimen shall be ground in the usual manner on 240, 400, and 600 grit silicon carbide papers. The scratches from the last paper shall then be removed by polishing with 30, 15, and 6 micron diamond abrasives for short times on a hard-finish cloth (i.e., unbleached muslin, Premier suede drill cloth, etc.). The mechanical polish shall be completed with very light pressure on a short-pile cloth (i.e., Buehler Microcloth) charged with a thick slurry of Linde alumina abrasive and water.

Cathodic Vacuum Etching: The specimen shall then be cathodic vacuum etched, using 1500 volts at a pressure of 300 microns of argon. The etching shall be done in 30 second intervals, each interval followed by a 30 to 60 second cooling period, until the microstructure is fully revealed. The total etching time will vary from specimen to specimen, but should be within the range of 3 to 10 minutes.

APPENDIX III

Complete X-ray Diffraction Data

NASV-9 (Ta-9W-1Hf-0.025C)

As-Rolled

d	Intensity	Phase
3.15	VW	HfO ₂
2.82	VW	HfO ₂
2.69	M	HCP
2.62	VW	$\beta(2.37\text{Ta}_2\text{C})$
2.465	M	HCP
2.37	VS	HCP
1.82	M	HCP
1.553	M	HCP
1.405	M	HCP
1.345	W	HCP
1.316	M	HCP
1.298	MW	HCP
1.237	W	HCP
1.183	W	HCP
1.125	W	HCP
1.043	MW	HCP
1.018	VW	HCP
0.997	MW	HCP
0.967	MW	HCP
0.941	W	HCP
0.930	W	HCP
0.912	W	HCP
0.8975	W	HCP
0.867	MW	HCP
0.845	MW	HCP
0.7995	VW	HCP
0.787	VW	HCP
0.779	VW	HCP

NOTE:

HCP with $a_o = 3.11 \text{ \AA}$
 $c_o = 4.95 \text{ \AA}$
 $c/a = 1.59$
 assumed to be $(\text{Ta}, \text{W}, \text{Hf})_2\text{C}_{1-x}$

NASV-9 (Ta-9W-1Hf-0.025C)

As-Rolled + 1 Hr. at 1200°C/2190°F

d	Intensity	Phase
3.15	VW	HfO ₂
2.95	VW	?
2.82	VW	HfO ₂
2.69	M	HCP
2.62	VW	$\beta(2.37\text{Ta}_2\text{C})$
2.47	M	HCP
2.37	VS	HCP
1.82	M	HCP
1.554	M	HCP
1.408	M	HCP
1.345	W	HCP
1.316	M	HCP
1.298	MW	HCP
1.237	W	HCP
1.183	W	HCP
1.125	W	HCP
1.043	MW	HCP
1.018	W	HCP
0.997	M	HCP
0.967	MW	HCP
0.941	MW	HCP
0.9295	MW	HCP
0.911	W	HCP
0.8975	W	HCP
0.867	M	HCP
0.845	M	HCP
0.7995	W	HCP
0.787	W	HCP
0.7785	W	HCP

NOTE:

HCP with $a_o = 3.11 \text{ \AA}$
 $c_o = 4.95 \text{ \AA}$
 $c/a = 1.59$
 assumed to be $(\text{Ta}, \text{W}, \text{Hf})_2\text{C}_{1-x}$

NASV-9 (Ta-9W-1Hf-0.025C)

As-Rolled + 1 Hr. at 1400°C/2550°F

d	Intensity	Phase
3.15	VW	HfO ₂
2.97	VW	$\beta(2.69\text{Ta}_2\text{C})$
2.82	VW	HfO ₂
2.69	M	HCP
2.62	W	$\beta(2.37\text{Ta}_2\text{C})$
2.37	VS	HCP
2.20	VW	HfO ₂
2.02	VW	$\beta(1.82\text{Ta}_2\text{C})$
1.82	M	HCP
1.72	VW	$\beta(1.585\text{Ta}_2\text{C})$
1.64	VW	HfO ₂
1.555	M	HCP
1.407	M	HCP
1.345	W	HCP
1.317	M	HCP
1.299	M	HCP
1.238	W	HCP
1.183	W	HCP
1.125	W	HCP
1.043	M	HCP
1.018	W	HCP
0.997	S	HCP
0.969	M	HCP
0.942	MW	HCP
0.930	M	HCP
0.912	W	HCP
0.8975	MW	HCP
0.867	S	HCP
0.8455	MS	Ta ₂ C
0.837	VW	Ta ₂ C
0.799	MS	Ta ₂ C
0.7908	VW	Ta ₂ C
0.7875	M	Ta ₂ C
0.7787	M	Ta ₂ C

NOTE:

HCP with $a_o = 3.11 \text{ \AA}$
 $c_o = 4.95 \text{ \AA}$
 $c/a = 1.59$
 assumed to be $(\text{Ta}, \text{W}, \text{Hf})_2\text{C}_{1-x}$

NASV-9 (Ta-9W-1Hf-0.025C)
As-Rolled + 1 Hr. at 1600°C/2910°F

<u>d</u>	<u>Intensity</u>	<u>Phase</u>
2.69	M	HCP
2.47	M	HCP
2.37	VS	HCP
1.81	M	HCP
1.555	M	HCP
1.41	M	HCP
1.345	W	HCP
1.320	M	HCP
1.300	W	HCP
1.240	W	HCP
1.180	W	HCP
1.125	W	HCP
1.045	M	HCP
1.018	W	HCP
0.998	S	HCP
0.970	M	HCP
0.942	MW	HCP
0.932	M	HCP
0.899	MW	HCP
0.867	S	HCP
0.846	MS	HCP
0.800	MS	HCP
0.788	M	HCP
0.779	MW	HCP

NOTE:

HCP with $a_o = 3.11 \text{ \AA}$
 $c_o = 4.96 \text{ \AA}$
 $c/a = 1.59$

assumed to be $(\text{Ta,W,Hf})_2\text{C}_{1-x}$

NASV-9 (Ta-9W-1Hf-0.025C)
As-Rolled + 1 Hr. at 1800°C/3270°F

<u>d</u>	<u>Intensity</u>	<u>Phase</u>
2.68	M	HCP
2.45	M	HCP
2.35	VS	HCP
1.81	M	HCP
1.55	M	HCP
1.40	M	HCP
1.34	W	HCP
1.31	M	HCP
1.295	W	HCP
1.230	W	HCP
1.178	W	HCP
1.120	W	HCP
1.039	M	HCP
1.015	W	HCP
0.992	S	HCP
0.965	M	HCP
0.937	MW	HCP
0.925	M	HCP
0.895	MW	HCP
0.863	S	HCP
0.840	MS	HCP

NOTE:

HCP with $a_o = 3.10 \text{ \AA}$
 $c_o = 4.92 \text{ \AA}$
 $c/a = 1.59$

assumed to be $(\text{Ta,W,Hf})_2\text{C}_{1-x}$
 Lines are broad and diffuse.

NASV-9 (Ta-9W-1Hf-0.025C)
As-Rolled + 1 Hr. at 2000°C/3630°F

<u>d</u>	<u>Intensity</u>	<u>Phase</u>
2.68	M	HCP
2.45	M	HCP
2.35	VS	HCP
1.81	M	HCP
1.55	M	HCP
1.40	M	HCP
1.34	W	HCP
1.31	M	HCP
1.295	W	HCP
1.230	W	HCP
1.178	W	HCP
1.120	W	HCP
1.039	M	HCP
1.015	W	HCP
0.992	S	HCP
0.965	M	HCP
0.937	MW	HCP
0.925	M	HCP
0.895	MW	HCP
0.863	S	HCP
0.840	MS	HCP

NOTE:

HCP with $a_o = 3.10 \text{ \AA}$
 $c_o = 4.92 \text{ \AA}$
 $c/a = 1.59$

assumed to be $(\text{Ta,W,Hf})_2\text{C}_{1-x}$
 Lines are broad and diffuse.

NASV-9 (Ta-9W-1Hf-0.025C)

As-Rolled + 1 Hr. at 1600°C/2910°F
+ 506 Hrs. at 1315°C/2400°F

<u>d</u>	<u>Intensity</u>	<u>Phase</u>
3.15	W	HfO ₂
2.97	W	β(2.69Ta ₂ C)
2.82	W	HfO ₂
2.69	M	HCP
2.63	MW	β(2.37Ta ₂ C)
2.465	M	HCP
2.37	VS	HCP
2.20	VW	HfO ₂
2.07	VVVW	?
2.02	VVW	β(1.82Ta ₂ C)
1.88	VVW	?
1.82	M	HCP
1.72	VVW	β(1.555Ta ₂ C)
1.65	VVVW	?
1.553	M	HCP
1.405	M	HCP
1.345	W	HCP
1.316	M	HCP
1.298	MW	HCP
1.237	W	HCP
1.183	W	HCP
1.125	W	HCP
1.043	MW	HCP
1.018	VW	HCP
0.997	MW	HCP
0.967	MW	HCP
0.941	W	HCP
0.930	W	HCP
0.912	W	HCP
0.8975	W	HCP
0.867	MW	HCP
0.845	MW	HCP
0.7995	VW	HCP
0.787	VW	HCP
0.779	VW	HCP

NOTE:
HCP with $a_o = 3.11 \text{ \AA}$
 $c_o = 4.95 \text{ \AA}$
 $c/a = 1.59$

assumed to be (Ta,W,Hf)₂C_{1-x}

NASV-9 (Ta-9W-1Hf-0.025C)

As-Rolled + 1 Hr. at 1800°C/3270°F
+ 506 Hrs. at 1315°C/2400°F

<u>d</u>	<u>Intensity</u>	<u>Phase</u>
3.15	VVW	HfO ₂
2.97	VVW	β(2.69Ta ₂ C)
2.82	VVW	HfO ₂
2.69	S	HCP
2.62	MW	β(2.37Ta ₂ C)
2.47	S	HCP
2.37	VVS	HCP
2.20	VVW	HfO ₂
2.07	VVW	?
2.02	VVW	β(1.82Ta ₂ C)
1.875	W	?
1.82	S	HCP
1.72	VVW	β(1.555Ta ₂ C)
1.555	S	HCP
1.460	VVW	HfO ₂
1.440	VVW	β(1.306Ta ₂ C)
1.408	S	HCP
1.385	VVW	?
1.306	S	HCP
1.300	S	HCP
1.238	M	HCP
1.183	W	HCP
1.125	W	HCP
1.043	M	HCP
1.018	W	HCP
0.997	S	HCP
0.969	M	HCP
0.942	MW	HCP
0.930	M	HCP
0.912	W	HCP
0.8975	MW	HCP
0.867	S	HCP
0.8455	MS	HCP
0.837	VW	HCP
0.799	MS	HCP
0.7908	VW	HCP
0.7875	M	HCP
0.7787	M	HCP

NOTE:
HCP with $a_o = 3.11 \text{ \AA}$
 $c_o = 4.95 \text{ \AA}$
 $c/a = 1.59$

assumed to be (Ta,W,Hf)₂C_{1-x}

NASV-9 (Ta-9W-1Hf-0.025C)

As-Rolled + 1 Hr. at 2000°C/3630°F
+ 506 Hrs. at 1315°C/2400°F

<u>d</u>	<u>Intensity</u>	<u>Phase</u>
3.15	VVW	HfO ₂
2.97	VVW	β(2.69Ta ₂ C)
2.82	VVW	HfO ₂
2.69	S	HCP
2.62	MW	β(2.37Ta ₂ C)
2.47	S	HCP
2.37	VVS	HCP
2.20	VVW	HfO ₂
2.07	VVW	?
2.02	VVW	β(1.82Ta ₂ C)
1.88	VVW	?
1.875	W	?
1.82	S	HCP
1.72	VVW	β(1.555Ta ₂ C)
1.555	S	HCP
1.460	VVW	HfO ₂
1.440	VVW	β(1.306Ta ₂ C)
1.408	S	HCP
1.385	VVW	?
1.306	S	HCP
1.300	S	HCP
1.238	M	HCP
1.183	W	HCP
1.125	W	HCP
1.043	M	HCP
1.018	W	HCP
0.997	S	HCP
0.969	M	HCP
0.942	MW	HCP
0.930	M	HCP
0.912	W	HCP
0.8975	MW	HCP
0.867	S	HCP
0.8455	MS	HCP
0.837	VW	HCP
0.799	MS	HCP
0.7908	VW	HCP
0.7875	M	HCP
0.7787	M	HCP

NOTE:
HCP with $a_o = 3.11 \text{ \AA}$; $c_o = 4.95 \text{ \AA}$;
 $c/a = 1.59$; assumed to be (Ta,W,Hf)₂
C_{1-x}.

NASV-9 (Ta-9W-1Hf-0.025C)
1 hr. at 1650°C/3000°F + 210 hrs. at
1315°C/2400°F and 15,000 psi

<u>d</u>	<u>Intensity</u>	<u>Phase</u>
3.15	VW	HfO ₂
2.95	VW	
2.82	VW	HfO ₂
2.68	M	HCP
2.62	W	β(2.37Ta ₂ C)
2.47	M	HCP
2.37	VS	HCP
2.32	VW	HfO ₂
1.98	VW	HfO ₂
1.82	M	HCP
1.72	VW	β(1.55Ta ₂ C)
1.64	VW	HfO ₂
1.55	M	HCP
1.41	M	HCP
1.345	W	HCP
1.315	M	HCP
1.300	M	HCP
1.238	W	HCP
1.183	W	HCP
1.125	W	HCP
1.043	MW	HCP
1.018	W	HCP
0.997	MS	HCP
0.970	MW	HCP
0.942	MW	HCP
0.930	MW	HCP
0.912	W	HCP
0.898	W	HCP
0.868	M	HCP
0.844	MW	HCP
0.800	W	HCP
0.788	W	HCP
0.778	W	HCP

NOTE:
HCP with $a_o = 3.11 \text{ \AA}$
 $c_o = 4.96 \text{ \AA}$
 $c/a = 1.59$
assumed to be (Ta,W,Hf)₂C_{1-x}

NASV-9 (Ta-9W-1Hf-0.025C)
1 hr. at 1800°C/3270°F + 500 hrs. at
1315°C/2400°F and 15,000 psi

<u>d</u>	<u>Intensity</u>	<u>Phase</u>
2.70	M	HCP
2.62	VW	β(2.37Ta ₂ C)
2.47	M	HCP
2.36	VS	HCP
1.98	VW	HfO ₂
1.825	M	HCP ²
1.56	M	HCP
1.41	M	HCP
1.35	VW	HCP
1.32	M	HCP
1.30	MW	HCP
1.24	VW	HCP
1.185	VW	HCP
1.13	VW	HCP
1.045	MW	HCP
1.020	VW	HCP
0.998	MW	HCP
0.980	W	HCP
0.942	W	HCP
0.930	W	HCP
0.900	W	HCP
0.868	MW	HCP
0.846	W	HCP

NOTE:
HCP with $a_o = 3.11 \text{ \AA}$
 $c_o = 4.96 \text{ \AA}$
 $c/a = 1.59$
assumed to be (Ta,W,Hf)₂C_{1-x}

NASV-2 (8W-2Hf-0.05C)
1 hr. at 1650°C/3000°F + 96 hrs.
at 1315°C/2400°F and 14,095 psi

<u>d</u>	<u>Intensity</u>	<u>Phase</u>
2.70	M	HCP
2.64	M	FCC
2.48	M	HCP
2.375	VS	HCP
2.29	M	FCC
1.83	M	HCP
1.62	MW	FCC
1.56	M	HCP
1.415	M	HCP
1.375	MW	FCC
1.35	W	HCP
1.322	M	HCP
1.305	M	HCP
1.245	W	HCP
1.188	W	HCP
1.150	W	FCC
1.13	MW	HCP
1.054	W	HCP
1.047	M	FCC
1.029	W	FCC
1.022	W	HCP
1.000	S	HCP
0.972	M	HCP
0.945	M	HCP
0.938	VW	FCC
0.935	M	HCP
0.915	W	HCP
0.900	M	HCP
0.885	W	FCC
0.870	S	HCP
0.848	MS	HCP
0.840	VW	HCP
0.813	VW	HCP
0.802	W	HCP
0.790	W	HCP
0.781	W	HCP
0.777	W	HCP

NOTE:
HCP with $a_o = 3.12 \text{ \AA}$
 $c_o = 4.98 \text{ \AA}$
 $c/a = 1.60$
assumed to be (Ta,W,Hf)₂C_{1-x}
FCC with $a_o = 4.60 \text{ \AA}$
assumed to be (Hf,Ta)C_{1-x}

NAS-27 (4.6W-1.5Hf-.05C)
1 hr. at 1650°C/3000°F + 76 hrs. at
1315°C/2400°F and 10,000 psi

d	Intensity	Phase
3.15	VVW	HfO ₂
2.82	W	HfO ₂
2.69	M	HCP
2.62	VW	β(2.37Ta ₂ C) +FCC
2.465	M	HCP
2.42	W	HCP
2.37	VS	HCP
2.29	W	FCC
2.02	VVVW	HfO ₂
1.82	M	HCP
1.72	VVW	β(1.555Ta ₂ C)
1.65	W	HfO ₂
1.62	VW	FCC
1.553	M	HCP
1.405	M	HCP
1.385	VW	FCC
1.345	W	HCP
1.316	M	HCP
1.298	MW	HCP
1.237	W	HCP
1.183	W	HCP
1.125	W	HCP
1.043	MW	HCP
1.018	VW	HCP
0.997	MW	HCP
0.967	MW	HCP
0.941	W	HCP
0.930	W	HCP
0.912	W	HCP
0.8975	W	HCP
0.867	MW	HCP
0.845	MW	HCP
0.7995	VW	HCP
0.787	VW	HCP
0.779	VW	HCP

NOTE:

HCP with $a_o = 3.11 \text{ \AA}$; $c_o = 4.95 \text{ \AA}$;
 $c/a = 1.59$; assumed to be (Ta,W,Hf)₂
C_{1-x}. Lines of HCP phase are very
broad in back reflection indicating
solid solution or variable composition
of C/Ta.
FCC with $a_o = 4.58 \text{ \AA}$ assumed to be
(Hf,Ta)C.

NAS-21 (8.6W-.53Hf-.02C)
1 hr. at 1650°C/3000°F + 96 hrs.
at 1315°C/2400°F and 15,070 psi

d	Intensity	Phase
2.69	M	HCP
2.465	M	HCP
2.37	VS	HCP
1.98	VVW	HfO ₂
1.82	M	HCP
1.553	M	HCP
1.405	M	HCP
1.345	W	HCP
1.316	M	HCP
1.298	MW	HCP
1.237	W	HCP
1.183	W	HCP
1.125	W	HCP
1.043	MW	HCP
1.018	VW	HCP
0.997	MW	HCP
0.967	MW	HCP
0.941	W	HCP
0.930	W	HCP
0.912	W	HCP
0.8975	W	HCP
0.867	MW	HCP
0.845	MW	HCP
0.7995	VW	HCP
0.787	VW	HCP
0.779	VW	HCP

NOTE:

HCP with $a_o = 3.11 \text{ \AA}$;
 $c_o = 4.95 \text{ \AA}$;
 $c/a = 1.59$
assumed to be (Ta,W,Hf)₂C_{1-x}

T-111 (8W-2Hf)
1 hr. at 1650°C/3000°F + 172 hrs.
at 1370°C/2500°F and 7,650 psi and
5 x 10⁻⁶ torr

d	Intensity	Phase
5.00	VW	HfO ₂
4.10	VW	HfO ₂
3.65	M	HfO ₂
3.12	S	HfO ₂
2.92β	W	HfO ₂
2.82	MS	HfO ₂
2.65	VS	FCC
2.60	MW	HfO ₂
2.53	MW	HfO ₂
2.46	W	HfO ₂
2.30	S	FCC
2.36	MW	HfO ₂
2.20	MW	HfO ₂
2.17	W	HfO ₂
2.00	W	HfO ₂
1.97	W	HfO ₂
1.835	MW	HfO ₂
1.800	M	HfO ₂
1.765	VW	HfO ₂
1.680	MW	HfO ₂
1.650	W	FCC
1.625	S	FCC
1.385	S	FCC
1.325	M	FCC
1.150	W	FCC
1.055	MS	FCC
1.030	MS	FCC
0.940	MS	FCC
0.887	MS	FCC
0.814	M	FCC
0.778	MS	FCC

NOTE:

FCC with $a_o = 4.60 \text{ \AA}$
assumed to be (Hf,Ta,W)C_{1-x}

NAS-56 (8W-1Re-7Hf-.025C)
1 hr. at 1650°C/3000°F + 193 hrs.
at 1315°C/2400°F and 12,690 psi

d	Intensity	Phase
3.15	VVW	HfO ₂
2.82	VVVW	HfO ₂
2.69	M	HCP
2.62	VVW	β(2.37Ta ₂ C)
2.47	S	HCP
2.37	VS	HCP
1.82	MS	HCP
1.555	MS	HCP
1.405	MS	HCP
1.345	W	HCP
1.315	MS	HCP
1.300	M	HCP
1.2355	W	HCP
1.183	W	HCP
1.125	W	HCP
1.042	M	HCP
1.028	W	HCP
0.997	MS	HCP
0.968	M	HCP
0.941	MW	HCP
0.929	MW	HCP
0.910	W	HCP
0.897	W	HCP
0.867	MS	HCP
0.844	M	HCP
0.796	M	HCP
0.7875	VW	HCP
0.796	W	HCP
0.776	W	HCP

NOTE:
HCP with $a_o = 3.11 \text{ \AA}$
 $c_o = 4.95 \text{ \AA}$
 $c/a = 1.59$
assumed to be (Ta,W,Hf)₂C_{1-x}

NAS-56 (8W-1Re-7Hf-.025C)
1 hr. at 1650°C/3000°F + 308 hrs.
at 1315°C/2400°F and 15,000 psi

d	Intensity	Phase
2.69	M	HCP
2.62	VVW	β(2.37Ta ₂ C)
2.47	S	HCP
2.37	VS	HCP
1.82	MS	HCP
1.555	MS	HCP
1.405	MS	HCP
1.345	W	HCP
1.315	MS	HCP
1.300	M	HCP
1.2355	W	HCP
1.183	W	HCP
1.125	W	HCP
1.042	M	HCP
1.028	W	HCP
0.997	MS	HCP
0.968	M	HCP
0.941	MW	HCP
0.929	MW	HCP
0.910	W	HCP
0.897	W	HCP
0.867	MS	HCP
0.844	M	HCP
0.796	M	HCP
0.7875	VW	HCP
0.796	W	HCP
0.776	W	HCP

NOTE:
HCP with $a_o = 3.11 \text{ \AA}$
 $c_o = 4.95 \text{ \AA}$
 $c/a = 1.59$
assumed to be (Ta,W,Hf)₂C_{1-x}

NASV-4 (8W-2.7Hf-.4Zr-.05C)
1 hr. at 1650°C/3000°F + 70 hrs.
at 1315°C/2400°F and 14,000 psi

d	Intensity	Phase
2.94	VW	FCC ₃
2.64	VS	FCC ₁ & 2
2.53	VW	FCC ₃
2.29	S	FCC ₁ & 2
1.98	VW	HfO ₂
1.80	VW	FCC ₃
1.62	S	FCC ₁ & 2
1.535	VVW	FCC ₃
1.47	VVVW	?
1.388	M	FCC ₁
1.380	M	FCC ₂
1.360	VVW	?
1.329	MW	FCC ₁
1.320	MW	FCC ₂
1.151	W	FCC ₁
1.145	W	FCC ₂
1.058	M	FCC ₁
1.050	M	FCC ₂
1.030	M	FCC ₁
1.023	M	FCC ₂
0.941	M	FCC ₁
0.934	M	FCC ₂
0.8875	M	FCC ₁
0.888	M	FCC ₂
0.815	W	FCC ₁
0.800	W	FCC ₂
0.7795	MW	FCC ₁
0.774	MW	FCC ₂

NOTE:
FCC₁ with $a_o = 4.61 \text{ \AA}$
FCC₂ with $a_o = 4.58 \text{ \AA}$

Above two FCC phases are assumed to be the monocarbides of Hf and Zr, having carbon deficiencies, substitution of Ta for Hf and Zr, etc.
FCC₃ with $a_o = 5.10 \text{ \AA}$. Tentatively identified as the cubic form of ZrO₂.

NAS-42 (Ta-5.3W-1.56 Re-0.65Mo-
0.52 Zr-0.08N)

Annealed 1 hr at 1650°C/3000°F

d	Intensity	Phase
2.95	VW	FCC ₂
2.64	MS	FCC ₁
2.53	VW	FCC ₂
2.28	MS	FCC ₁
1.81	VW	FCC ₂
1.615	M	FCC ₁
1.530	VW	FCC ₂
1.380	M	FCC ₁
1.320	W	FCC ₁
1.145	VW	FCC ₁
1.050	W	FCC ₁
1.023	MW	FCC ₁
0.935	MW	FCC ₁
0.882	MW	FCC ₁
0.810	VW	FCC ₁
0.775	MW	FCC ₁

NOTE:

FCC₁ with $a_o = 4.57 \text{ \AA}$
assumed to be ZrN

FCC₂ with $a_o = 5.10 \text{ \AA}$
tentatively identified as
the cubic form of ZrO₂

NAS-42 (Ta-5.3W - 1.56 Re-0.65 Mo-
0.52 Zr-0.08N)

1 hr. at 1650°C/3000°F + 180 hrs. at
1315°C/2400°F, 24 hrs. at 1370°C/
2500°F and 20,000 psi

d	Intensity	Phase
2.95	VW	FCC ₂
2.64	MS	FCC ₁
2.53	VW	FCC ₂
2.28	MS	FCC ₁
1.81	VW	FCC ₂
1.615	M	FCC ₁
1.530	VW	FCC ₂
1.380	M	FCC ₁
1.320	W	FCC ₁
1.145	VW	FCC ₁
1.050	W	FCC ₁
1.023	MW	FCC ₁
0.935	MW	FCC ₁
0.882	MW	FCC ₁
0.810	VW	FCC ₁
0.775	MW	FCC ₁

NOTE:

FCC₁ with $a_o = 4.57 \text{ \AA}$
assumed to be ZrN

FCC₂ with $a_o = 5.10 \text{ \AA}$
tentatively identified as
the cubic form of ZrO₂

NASV-7 (Ta-5.7W - 1.56 Re-0.7 Mo-
0.25 Hf - 0.13 Zr - 0.015C - 0.015N)

As-Rolled

d	Intensity	Phase
3.15	VW	HfO ₂
2.82	VW	HfO ₂
2.68	M	HCP ²
2.45	M	HCP
2.35	VS	HCP
1.81	M	HfO ₂
1.81	M	HCP
1.55	M	HCP
1.40	M	HCP
1.34	VW	HCP
1.31	M	HCP
1.295	M	HCP
1.230	W	HCP
1.178	W	HCP
1.120	W	HCP
1.039	MW	HCP
1.015	VW	HCP
0.992	M	HCP
0.965	M	HCP
0.937	W	HCP
0.925	W	HCP
0.895	W	HCP
0.863	M	HCP
0.840	W	HCP

NOTE:

HCP $a_o = 3.10 \text{ \AA}$, $c_o = 4.92 \text{ \AA}$,
 $\phi/a = 1.59$ assumed to be (Ta, W,
Hf)₂C_{1-x}
Lines are broad and diffuse

NASV-7

As-Rolled + 1 hour at 1200°C/2190°F

d	Intensity	Phase
3.15	W	HfO ₂
2.97	VW	$\beta(2.69 \text{ Ta}_2\text{C})$
2.82	W	HfO ₂
2.68	S	HCP
2.62	W	$\beta(2.37 \text{ Ta}_2\text{C})$
2.47	S	HCP
2.37	VS	HCP
2.02	VVW	$\beta(1.82 \text{ Ta}_2\text{C})$
1.81	S	HCP
1.72	W	$\beta(1.55 \text{ Ta}_2\text{C})$
1.68	W	HfO ₂
1.64	VW	HfO ₂
1.55	S	HCP
1.405	S	HCP
1.342	MW	HCP
1.314	S	HCP
1.295	S	HCP
1.235	MW	HCP
1.180	MW	HCP
1.123	MW	HCP
1.040	M	HCP
1.015	W	HCP
0.995	MS	HCP
0.967	M	HCP
0.940	MW	HCP
0.928	MW	HCP
0.910	W	HCP
0.897	MW	HCP
0.865	MS	HCP
0.843	M	HCP
0.824	W	HCP
0.7965	MW	HCP
0.785	W	HCP
0.7765	W	HCP

NOTE:

HCP $a_o = 3.10 \text{ \AA}$, $c_o = 4.94 \text{ \AA}$, $c/a = 1.59$
assumed to be $(\text{Ta}, \text{W}, \text{Hf})_2\text{C}_{1-x}$

NASV-7

As-Rolled + 1 hour at 1400°C/2550°F

d	Intensity	Phase
3.15	M	HfO ₂
2.95	VVW	FCC
2.82	M	HfO ₂
2.69	M	HCP
2.60	M	HfO ₂
2.465	M	HCP
2.37	VS	HCP
2.20	VW	HfO ₂
1.88	VVW	? ₂
1.72	VVW	$\beta(1.553 \text{ Ta}_2\text{C})$
1.685	VVW	HfO ₂
1.64	VW	HfO ₂
1.553	M	HCP
1.405	M	HCP
1.345	W	HCP
1.316	M	HCP
1.298	MW	HCP
1.237	W	HCP
1.183	W	HCP
1.125	W	HCP
1.043	MW	HCP
1.018	VW	HCP
0.997	MW	HCP
0.967	MW	HCP
0.941	W	HCP
0.930	W	HCP
0.912	W	HCP
0.8975	W	HCP
0.867	MW	HCP
0.845	MW	HCP
0.7995	VW	HCP
0.787	VW	HCP
0.779	VW	HCP

NOTE:

HCP $a_o = 3.11 \text{ \AA}$, $c_o = 4.95 \text{ \AA}$, $c/a = 1.59$
assumed to be $(\text{Ta}, \text{W}, \text{Hf})_2\text{C}_{1-x}$

FCC $a_o = 5.10 \text{ \AA}$
tentatively identified as the
cubic form of ZrO_2

NASV-7

As-Rolled + 1 hour at 1600°C/2910°F

d	Intensity	Phase
3.15	W	HfO ₂
2.95	MW	FCC
2.82	VW	HfO ₂
2.68	M	HCP
2.60	VW	HfO ₂
2.52	VVW	FCC
2.45	M	HCP
2.35	S	HCP
1.81	M	HCP
1.55	M	HCP
1.54	VVW	FCC
1.47	VVW	FCC
1.40	M	HCP
1.34	VW	HCP
1.31	M	HCP
1.295	M	HCP
1.230	VW	HCP
1.178	VW	HCP
1.120	VVW	HCP
1.039	MW	HCP
1.015	VVW	HCP
0.992	M	HCP
0.965	MW	HCP
0.937	W	HCP
0.925	W	HCP
0.895	VW	HCP
0.863	MW	HCP
0.840	VW	HCP

NOTE:

HCP $a_o = 3.10 \text{ \AA}$, $c_o = 4.92 \text{ \AA}$, $c/a = 1.59$
assumed to be $(\text{Ta}, \text{W}, \text{Hf})_2\text{C}_{1-x}$

FCC $a_o = 5.10 \text{ \AA}$
tentatively identified as the cubic form of
 ZrO_2

NASV-7

As-Rolled + 1 Hour at 1800°C/3270°F

d	Intensity	Phase
2.69	M	HCP
2.57	VW	HCP
2.47	M	HCP
2.37	S	HCP-BCC ₂
2.34	S	BCC ₁
1.82	M	HCP
1.69	M	BCC ₂
1.65	M	BCC ₁
1.55	M	HCP
1.405	W	HCP
1.380	M	BCC ₂
1.350	M	BCC ₁
1.315	W	HCP
1.295	W	HCP
1.195	W	BCC ₂
1.182	VW	HCP ²
1.170	W	BCC ₁
1.070	W	BCC ₂
1.045	VW	BCC ₁
0.995	VW	HCP
0.953	VW	BCC ₁
0.904	W	BCC ₂
0.883	M	BCC ₁
0.798	W	BCC ₂
0.7855	W	HCP ²

NOTE:

HCP $a_o = 3.11\text{\AA}$, $c_o = 4.95\text{\AA}$,
 $c/a = 1.59$
 assumed to be (Ta, W, Hf)₂C_{1-x}

BCC₁ $a_o = 3.30\text{\AA}$
 assumed to be Ta

BCC₂ $a_o = 3.38\text{\AA}$
 not presently identified

NASV-7

As-Rolled + 1 hour at 2000°C/3630°F

d	Intensity	Phase
2.65	M	BCC ₂
2.40	MS	BCC ₁
1.87	W	BCC ₂
1.695	W	BCC ₁
1.535	VW	BCC ₂
1.385	W	BCC ₁
1.200	VW	BCC ₁
1.075	VW	BCC ₁
0.907	W	BCC ₁

NOTE:

BCC₁ $a_o = 3.40\text{\AA}$
 BCC₂ $a_o = 3.74\text{\AA}$

above two BCC phases have not
 been identified

NASV-7

As-Rolled + 1 hour at 1600°C/2910°F

d	Intensity	Phase
3.15	VW	HfO ₂
2.95	VW	FCC ₂
2.82	VW	HfO ₂
2.69	MS	HCP
2.65	W	FCC ₁
2.54	VW	FCC ₂
2.47	MS	HCP
2.36	VS	HCP
2.30	MW	FCC ₁
1.99	VW	?
1.82	M	HCP
1.625	W	FCC ₁
1.555	M	HCP
1.405	M	HCP
1.385	W	FCC ₁
1.345	W	HCP
1.325	VW	FCC ₁
1.315	M	HCP
1.298	MW	HCP
1.237	W	HCP
1.183	W	HCP
1.150	VW	FCC ₁
1.055	W	FCC ₁
1.043	MW	HCP
1.028	W	FCC ₁
1.018	VW	HCP
0.997	MW	HCP
0.967	MW	HCP
0.941	W	HCP
0.930	W	HCP
0.912	W	HCP
0.8975	W	HCP
0.885	MW	FCC ₁
0.867	MW	HCP
0.845	MW	HCP
0.813	VW	FCC ₁

NOTE:

HCP $a_o = 3.11\text{\AA}$, $c_o = 4.95\text{\AA}$,
 $c/a = 1.59$ assumed to be (Ta, W,
 Hf)₂C_{1-x}

FCC₁ $a_o = 4.60\text{\AA}$ assumed to be ZrN

FCC₂ $a_o = 5.10\text{\AA}$ tentatively identi-
 fied as the cubic form of ZrO₂

NASV-7

As-Rolled + 1 hour at 1800°C/3270°F
+ 500 hours at 1315°C/2400°F

d	Intensity	Phase
2.68	MS	HCP
2.65	M	FCC
2.47	MS	HCP
2.36	VS	HCP
2.295	M	FCC
1.98	VVW	?
1.82	MS	HCP
1.625	M	FCC
1.55	MS	HCP
1.405	MS	HCP
1.385	M	FCC
1.342	W	HCP
1.328	VVW	FCC
1.315	MS	HCP
1.295	MS	HCP
1.235	W	HCP
1.180	M	HCP
1.150	V	FCC
1.122	W	HCP
1.070	VW	HCP
1.055	M	FCC
1.040	M	HCP
1.029	M	FCC
0.995	MS	HCP
0.965	M	HCP
0.940	MW	HCP
0.928	MW	HCP
0.910	W	HCP
0.885	W	HCP
0.866	MS	HCP
0.8435	M	HCP
0.825	VW	HCP
0.8135	VW	HCP
0.797	M	HCP
0.7883	W	HCP
0.7855	MW	HCP
0.777	M	HCP

NOTE:

HCP $a_0 = 3.11\text{\AA}$; $c_0 = 4.94\text{\AA}$,
 $c/a = 1.59$ assumed to be $(\text{Ta}, \text{W}, \text{Hf})_2$
 C_{1-x} . FCC $a_0 = 4.60\text{\AA}$ assumed
to be ZrN.

NASV-7

As-Rolled + 1 hour at 2000°C/3630°F
+ 500 hours at 1315°C/2400°F

d	Intensity	Phase
2.68	MS	HCP
2.65	M	FCC
2.47	S	HCP
2.36	VS	HCP
2.295	M	FCC
1.82	M	HCP
1.625	M	FCC
1.55	M	HCP
1.405	M	HCP
1.342	VW	HCP
1.315	M	HCP
1.295	M	HCP
1.235	W	HCP
1.180	W	HCP
1.122	VW	HCP
1.055	M	FCC
1.040	M	HCP
1.025	VVW	HCP
0.995	MS	HCP
0.965	M	HCP
0.940	W	HCP
0.928	W	HCP
0.910	W	HCP
0.866	M	HCP
0.8435	M	HCP

NOTE:

HCP $a_0 = 3.11\text{\AA}$; $c_0 = 4.94\text{\AA}$;
 $c/a = 1.59$. Assumed to be
 $(\text{Ta}, \text{W}, \text{Hf})_2\text{C}_{1-x}$
FCC $a_0 = 4.60\text{\AA}$, assumed to be
ZrN

NASV-7

1 hr. at 1650°C/3000°F + 190 hrs.
at 1315°C/2400°F and 15,000 psi

d	Intensity	Phase
3.15	VW	HfO ₂
2.92	W	
2.82	VW	HfO ₂
2.68	S	HCP
2.63	M	FCC
2.52	VVW	HfO ₂
2.47	S	HCP
2.36	VS	HCP
2.29	M	FCC
1.82	MS	HCP
1.645	VVW	HfO ₂
1.62	MW	FCC
1.55	MS	HCP
1.405	MS	HCP
1.385	W	FCC
1.342	MW	HCP
1.315	MS	?
1.295	M	HCP
1.235	MW	HCP
1.180	MW	HCP
1.122	MW	HCP
1.052	VVW	FCC
1.040	M	HCP
1.025	VW	FCC
1.015	W	HCP
0.995	MS	HCP
0.965	M	HCP
0.940	MW	HCP, FCC
0.928	M	HCP
0.910	W	HCP
0.866	M	HCP
0.8435	M	HCP
0.825	VW	HCP
0.797	MW	HCP
0.7883	W	HCP
0.7855	MW	HCP
0.777	M	HCP

NOTE:

HCP $a_0 = 3.11\text{\AA}$; $c_0 = 4.94\text{\AA}$;
 $c/a = 1.59$ assumed to be $(\text{Ta},$
 $\text{W}, \text{Hf})_2\text{C}_{1-x}$
FCC $a_0 = 4.58\text{\AA}$ assumed to
be ZrN

NASV-7

1 hr. at 1800°C/3270°F + 816 hrs. at
1315°C/2400°F and 15,000 psi

<u>d</u>	<u>Intensity</u>	<u>Phase</u>
3.15	W	HfO
2.94	W	FCC ₂
2.82	W	HfO ₂
2.68	MS	HCP ²
2.64	M	FCC ₁
2.53	W	HfO ₂
2.47	MS	HCP ²
2.36	VS	HCP
2.29	M	FCC ₁
1.82	M	HCP ¹
1.645	W	HfO ₂
1.62	MW	FCC ₁
1.55	M	HCP
1.47	VW	HfO ₂
1.44	VW	HfO ₂
1.405	M	HCP ²
1.385	MW	FCC ₁
1.342	MW	HCP
1.325	W	FCC ₁
1.315	M	HCP
1.290	M	HCP
1.235	W	HCP
1.180	W	HCP
1.162	W	?
1.148	W	FCC
1.124	W	HCP
1.052	W	FCC
1.040	M	HCP

NOTE:

HCP $a_o = 3.11 \text{ \AA}$, $c_o = 4.94 \text{ \AA}$, $c/a = 1.59$
assumed to be (Ta, W, Hf)₂C_{1-x}

FCC₁ $a_o = 4.58 \text{ \AA}$
assumed to be ZrN.

FCC₂ $a_o = 5.10 \text{ \AA}$
tentatively identified as the cubic form of
ZrO₂

NASV-8 (Ta-5.7W-1.56Re-0.7Mo-

0.75 Hf-0.13Zr-0.15C-0.15N) 1 hr. at
1650°C/3000°F. 400 hrs. at 1315°C/2400°F
and 13,340 psi

<u>d</u>	<u>Intensity</u>	<u>Phase</u>
3.15	VW	HfO ₂
2.94	W	FCC ₂
2.82	VW	HfO ₂
2.65	VS	FCC ₁
2.52	VW	FCC ₂
2.29	S	FCC ₁
1.80	VW	FCC ₂
1.62	M	FCC ₁
1.535	VW	FCC ₂
1.47	VW	FCC ₂
1.383	M	FCC ₁
1.340	VW	
1.325	MW	FCC ₁
1.165	VW	FCC ₂
1.147	W	FCC ₁
1.052	M	FCC ₁
1.039	VW	FCC ₂
1.027	M	FCC ₁
0.937	MW	FCC ₁
0.884	M	FCC ₁
0.812	W	FCC ₁
0.7765	MS	FCC ₁

NOTE:

FCC₁ $a_o = 4.59 \text{ \AA}$, assumed to be
(Hf, Zr) (C, N)

FCC₂ $a_o = 5.09 \text{ \AA}$, tentatively identified
as the cubic form of ZrO₂.

See N66-15343



WANL-PR(Q)-007

May 26, 1966

ERRATA

The following correction is applicable to WANL-PR(Q)-007 entitled "Development of Dispersion Strengthened Tantalum Base Alloy", prepared under Contract NAS 3-2542.

Page 43

Change NASV-18 (Ta-6W-1Mo-1Re-0.7Hf-0.025C) to
read as follows:

NASV-18 (Ta-5W-1Re-0.3Zr-0.025N)

Astronuclear Laboratory
Westinghouse Electric Corporation
Pittsburgh 36, Pa.